

---

# FIBER OPTICS

## 8.1 STEP-INDEX FIBERS

- A. Guided Rays
- B. Guided Waves
- C. Single-Mode Fibers

## 8.2 GRADED-INDEX FIBERS

- A. Guided Waves
- B. Propagation Constants and Velocities

## 8.3 ATTENUATION AND DISPERSION

- A. Attenuation
- B. Dispersion
- C. Pulse Propagation

Dramatic improvements in the development of low-loss materials for optical fibers are responsible for the commercial viability of fiber-optic communications. **Corning** Incorporated pioneered the development and manufacture of ultra-low-loss glass fibers.



C O R N I N G

An optical fiber is a cylindrical dielectric waveguide made of low-loss materials such as silica glass. It has a central **core** in which the light is guided, embedded in an outer **cladding** of slightly lower refractive index (Fig. 8.0-1). Light rays incident on the core-cladding boundary at angles greater than the critical angle undergo total internal reflection and are guided through the core without refraction. Rays of greater inclination to the fiber axis lose part of their power into the cladding at each reflection and are not guided.

As a result of recent technological advances in fabrication, light can be guided through 1 km of glass fiber with a loss as low as  $\approx 0.16$  dB ( $\approx 3.6\%$ ). Optical fibers are replacing copper coaxial cables as the preferred transmission medium for electromagnetic waves, thereby revolutionizing terrestrial communications. Applications range from long-distance telephone and data communications to computer communications in a local area network.

In this chapter we introduce the principles of light transmission in optical fibers. These principles are essentially the same as those that apply in planar dielectric waveguides (Chap. 7), except for the cylindrical geometry. In both types of waveguide light propagates in the form of modes. Each mode travels along the axis of the waveguide with a distinct propagation constant and group velocity, maintaining its transverse spatial distribution and its polarization. In planar waveguides, we found that each mode was the sum of the multiple reflections of a TEM wave bouncing within the slab in the direction of an optical ray at a certain bounce angle. This approach is approximately applicable to cylindrical waveguides as well. When the core diameter is small, only a single mode is permitted and the fiber is said to be a **single-mode fiber**. Fibers with large core diameters are **multimode fibers**.

One of the difficulties associated with light propagation in multimode fibers arises from the differences among the group velocities of the modes. This results in a variety of travel times so that light pulses are broadened as they travel through the fiber. This effect, called **modal dispersion**, limits the speed at which adjacent pulses can be sent without overlapping and therefore the speed at which a fiber-optic communication system can operate.

Modal dispersion can be reduced by grading the refractive index of the fiber core from a maximum value at its center to a minimum value at the core-cladding boundary. The fiber is then called a **graded-index fiber**, whereas conventional fibers

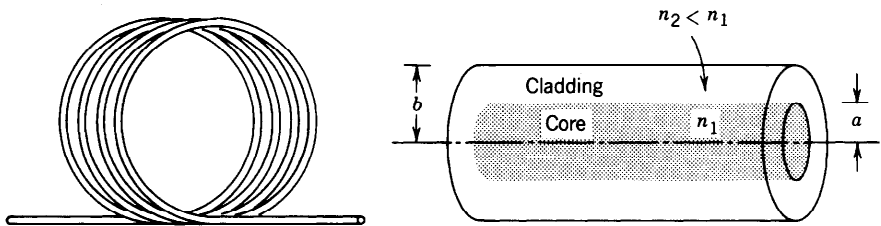


**Figure 8.0-1** An optical fiber is a cylindrical dielectric waveguide.

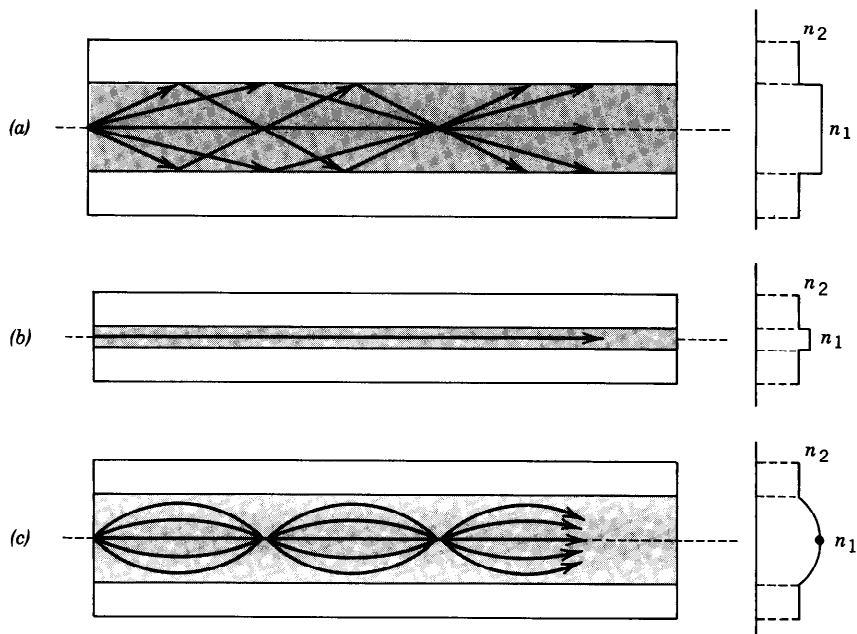


**Figure 8.0-2** Geometry, refractive-index profile, and typical rays in: (a) a multimode step-index fiber, (b) a single-mode step-index fiber, and (c) a multimode graded-index fiber.

with constant refractive indices in the core and the cladding are called **step-index fibers**. In a graded-index fiber the velocity increases with distance from the core axis (since the refractive index decreases). Although rays of greater inclination to the fiber axis must travel farther, they travel faster, so that the travel times of the different rays are equalized. Optical fibers are therefore classified as step-index or graded-index, and multimode or single-mode, as illustrated in Fig. 8.0-2.

This chapter emphasizes the nature of optical modes and their group velocities in step-index and graded-index fibers. These topics are presented in Secs. 8.1 and 8.2, respectively. The optical properties of the fiber material (which is usually fused silica), including its attenuation and the effects of material, modal, and waveguide dispersion on the transmission of light pulses, are discussed in Sec. 8.3. Optical fibers are revisited in Chap. 22, which is devoted to their use in lightwave communication systems.

### 8.1 STEP-INDEX FIBERS

A step-index fiber is a cylindrical dielectric waveguide specified by its core and cladding refractive indices,  $n_1$  and  $n_2$ , and the radii  $a$  and  $b$  (see Fig. 8.0-1). Examples of standard core and cladding diameters  $2a/2b$  are 8/125, 50/125, 62.5/125, 85/125, 100/140 (units of  $\mu\text{m}$ ). The refractive indices differ only slightly, so that the fractional refractive-index change

$$\Delta = \frac{n_1 - n_2}{n_1} \tag{8.1-1}$$

is small ( $\Delta \ll 1$ ).

Almost all fibers currently used in optical communication systems are made of fused silica glass ( $\text{SiO}_2$ ) of high chemical purity. Slight changes in the refractive index are

made by the addition of low concentrations of doping materials (titanium, germanium, or boron, for example). The refractive index  $n_1$  is in the range from 1.44 to 1.46, depending on the wavelength, and  $\Delta$  typically lies between 0.001 and 0.02.

## A. Guided Rays

An optical ray is guided by total internal reflections within the fiber core if its angle of incidence on the core-cladding boundary is greater than the critical angle  $\theta_c = \sin^{-1}(n_2/n_1)$ , and remains so as the ray bounces.

### Meridional Rays

The guiding condition is simple to see for meridional rays (rays in planes passing through the fiber axis), as illustrated in Fig. 8.1-1. These rays intersect the fiber axis and reflect in the same plane without changing their angle of incidence, as if they were in a planar waveguide. Meridional rays are guided if their angle  $\theta$  with the fiber axis is smaller than the complement of the critical angle  $\bar{\theta}_c = \pi/2 - \theta_c = \cos^{-1}(n_2/n_1)$ . Since  $n_1 \approx n_2$ ,  $\theta_c$  is usually small and the guided rays are approximately paraxial.

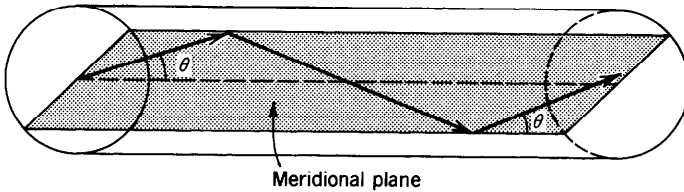


**Figure 8.1-1** The trajectory of a meridional ray lies in a plane passing through the fiber axis. The ray is guided if  $\theta < \bar{\theta}_c = \cos^{-1}(n_1/n_2)$ .

### Skewed Rays

An arbitrary ray is identified by its plane of incidence, a plane parallel to the fiber axis and passing through the ray, and by the angle with that axis, as illustrated in Fig. 8.1-2. The plane of incidence intersects the core-cladding cylindrical boundary at an angle  $\phi$  with the normal to the boundary and lies at a distance  $R$  from the fiber axis. The ray is identified by its angle  $\theta$  with the fiber axis and by the angle  $\phi$  of its plane. When  $\phi \neq 0$  ( $R \neq 0$ ) the ray is said to be skewed. For meridional rays  $\phi = 0$  and  $R = 0$ .

A skewed ray reflects repeatedly into planes that make the same angle  $\phi$  with the core-cladding boundary, and follows a helical trajectory confined within a cylindrical shell of radii  $R$  and  $a$ , as illustrated in Fig. 8.1-2. The projection of the trajectory onto the transverse ( $x$ - $y$ ) plane is a regular polygon, not necessarily closed. It can be shown that the condition for a skewed ray to always undergo total internal reflection is that its angle  $\theta$  with the  $z$  axis be smaller than  $\theta_c$ .

### Numerical Aperture

A ray incident from air into the fiber becomes a guided ray if upon refraction into the core it makes an angle  $\theta$  with the fiber axis smaller than  $\bar{\theta}_c$ . Applying Snell's law at the air-core boundary, the angle  $\theta_a$  in air corresponding to  $\bar{\theta}_c$  in the core is given by the relation  $1 \cdot \sin \theta_a = n_1 \sin \bar{\theta}_c$ , from which (see Fig. 8.1-3 and Exercise 1.2-5)  $\sin \theta_a = n_1(1 - \cos^2 \bar{\theta}_c)^{1/2} = n_1[1 - (n_2/n_1)^2]^{1/2} = (n_1^2 - n_2^2)^{1/2}$ . Therefore

$$\theta_a = \sin^{-1} \text{NA}, \quad (8.1-2)$$

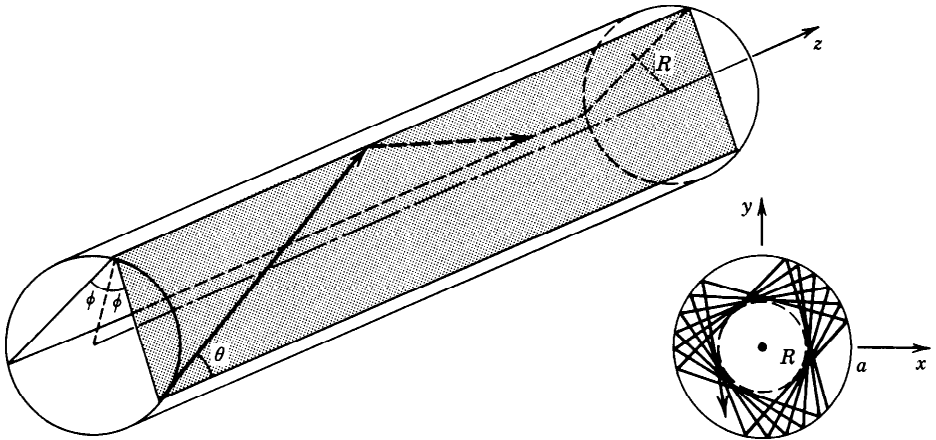


**Figure 8.1-2** A skewed ray lies in a plane offset from the fiber axis by a distance  $R$ . The ray is identified by the angles  $\theta$  and  $\phi$ . It follows a helical trajectory confined within a cylindrical shell of radii  $R$  and  $a$ . The projection of the ray on the transverse plane is a regular polygon that is not necessarily closed.

where

$$NA = (n_1^2 - n_2^2)^{1/2} \approx n_1(2\Delta)^{1/2} \tag{8.1-3}$$

Numerical Aperture

is the numerical aperture of the fiber. Thus  $\theta_a$  is the acceptance angle of the fiber. It

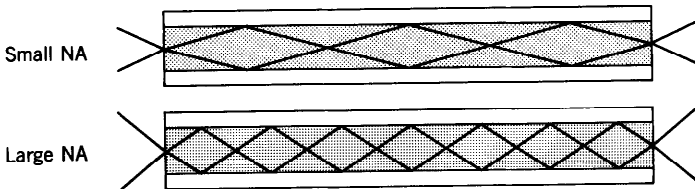
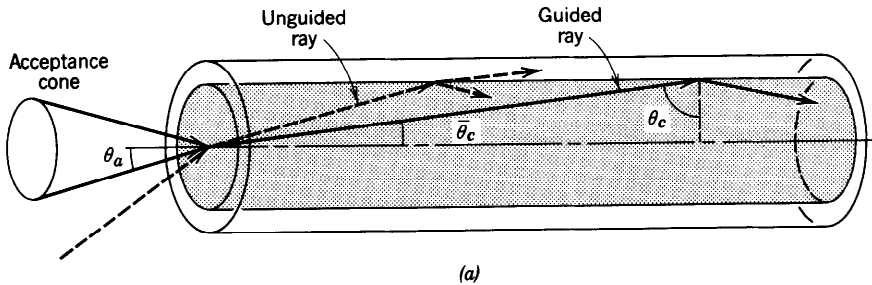


**Figure 8.1-3** (a) The acceptance angle  $\theta_a$  of a fiber. Rays within the acceptance cone are guided by total internal reflection. The numerical aperture  $NA = \sin \theta_a$ . (b) The light-gathering capacity of a large NA fiber is greater than that of a small NA fiber. The angles  $\theta_a$  and  $\theta_c$  are typically quite small; they are exaggerated here for clarity.

determines the cone of external rays that are guided by the fiber. Rays incident at angles greater than  $\theta_a$  are refracted into the fiber but are guided only for a short distance. The numerical aperture therefore describes the light-gathering capacity of the fiber.

When the guided rays arrive at the other end of the fiber, they are refracted into a cone of angle  $\theta_a$ . Thus the acceptance angle is a crucial parameter for the design of systems for coupling light into or out of the fiber.

---

**EXAMPLE 8.1-1. Cladded and Uncladded Fibers.** In a silica glass fiber with  $n_1 = 1.46$  and  $\Delta = (n_1 - n_2)/n_1 = 0.01$ , the complementary critical angle  $\bar{\theta}_c = \cos^{-1}(n_2/n_1) = 8.1^\circ$ , and the acceptance angle  $\theta_a = 11.9^\circ$ , corresponding to a numerical aperture  $\text{NA} = 0.206$ . By comparison, an uncladded silica glass fiber ( $n_1 = 1.46$ ,  $n_2 = 1$ ) has  $\bar{\theta}_c = 46.8^\circ$ ,  $\theta_a = 90^\circ$ , and  $\text{NA} = 1$ . Rays incident from *all* directions are guided by the uncladded fiber since they reflect within a cone of angle  $\bar{\theta}_c = 46.8^\circ$  inside the core. Although its light-gathering capacity is high, the uncladded fiber is not a suitable optical waveguide because of the large number of modes it supports, as will be shown subsequently.

---

## B. Guided Waves

In this section we examine the propagation of monochromatic light in step-index fibers using electromagnetic theory. We aim at determining the electric and magnetic fields of guided waves that satisfy Maxwell's equations and the boundary conditions imposed by the cylindrical dielectric core and cladding. As in all waveguides, there are certain special solutions, called modes (see Appendix C), each of which has a distinct propagation constant, a characteristic field distribution in the transverse plane, and two independent polarization states.

### Spatial Distributions

Each of the components of the electric and magnetic fields must satisfy the Helmholtz equation,  $\nabla^2 U + n^2 k_o^2 U = 0$ , where  $n = n_1$  in the core ( $r < a$ ) and  $n = n_2$  in the cladding ( $r > a$ ) and  $k_o = 2\pi/\lambda_o$  (see Sec. 5.3). We assume that the radius  $b$  of the cladding is sufficiently large that it can safely be assumed to be infinite when examining guided light in the core and near the core-cladding boundary. In a cylindrical coordinate system (see Fig. 8.1-4) the Helmholtz equation is

$$\frac{\partial^2 U}{\partial r^2} + \frac{1}{r} \frac{\partial U}{\partial r} + \frac{1}{r^2} \frac{\partial^2 U}{\partial \phi^2} + \frac{\partial^2 U}{\partial z^2} + n^2 k_o^2 U = 0, \quad (8.1-4)$$

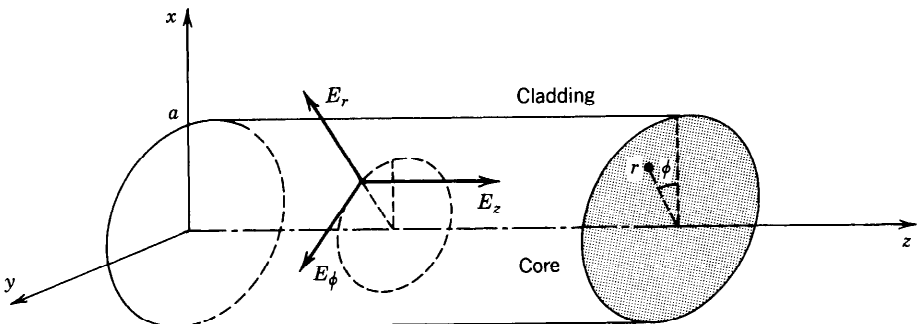


Figure 8.1-4 Cylindrical coordinate system.

where the complex amplitude  $U = U(r, \phi, z)$  represents any of the Cartesian components of the electric or magnetic fields or the axial components  $E_z$  and  $H_z$  in cylindrical coordinates.

We are interested in solutions that take the form of waves traveling in the  $z$  direction with a propagation constant  $\beta$ , so that the  $z$  dependence of  $U$  is of the form  $e^{-j\beta z}$ . Since  $U$  must be a periodic function of the angle  $\phi$  with period  $2\pi$ , we assume that the dependence on  $\phi$  is harmonic,  $e^{-jl\phi}$ , where  $l$  is an integer. Substituting

$$U(r, \phi, z) = u(r)e^{-jl\phi}e^{-j\beta z}, \quad l = 0, \pm 1, \pm 2, \dots, \quad (8.1-5)$$

into (8.1-4), an ordinary differential equation for  $u(r)$  is obtained:

$$\frac{d^2u}{dr^2} + \frac{1}{r} \frac{du}{dr} + \left( n^2k_o^2 - \beta^2 - \frac{l^2}{r^2} \right) u = 0. \quad (8.1-6)$$

As in Sec. 7.2B, the wave is guided (or bound) if the propagation constant is smaller than the wavenumber in the core ( $\beta < n_1k_o$ ) and greater than the wavenumber in the cladding ( $\beta > n_2k_o$ ). It is therefore convenient to define

$$k_T^2 = n_1^2k_o^2 - \beta^2 \quad (8.1-7a)$$

and

$$\gamma^2 = \beta^2 - n_2^2k_o^2, \quad (8.1-7b)$$

so that for guided waves  $k_T^2$  and  $\gamma^2$  are positive and  $k_T$  and  $\gamma$  are real. Equation (8.1-6) may then be written in the core and cladding separately:

$$\frac{d^2u}{dr^2} + \frac{1}{r} \frac{du}{dr} + \left( k_T^2 - \frac{l^2}{r^2} \right) u = 0, \quad r < a \text{ (core)}, \quad (8.1-8a)$$

$$\frac{d^2u}{dr^2} + \frac{1}{r} \frac{du}{dr} - \left( \gamma^2 + \frac{l^2}{r^2} \right) u = 0, \quad r > a \text{ (cladding)}. \quad (8.1-8b)$$

Equations (8.1-8) are well-known differential equations whose solutions are the family of Bessel functions. Excluding functions that approach  $\infty$  at  $r = 0$  in the core or at  $r \rightarrow \infty$  in the cladding, we obtain the bounded solutions:

$$u(r) \propto \begin{cases} J_l(k_T r), & r < a \text{ (core)} \\ K_l(\gamma r), & r > a \text{ (cladding)}, \end{cases} \quad (8.1-9)$$

where  $J_l(x)$  is the Bessel function of the first kind and order  $l$ , and  $K_l(x)$  is the modified Bessel function of the second kind and order  $l$ . The function  $J_l(x)$  oscillates like the sine or cosine functions but with a decaying amplitude. In the limit  $x \gg 1$ ,

$$J_l(x) \approx \left( \frac{2}{\pi x} \right)^{1/2} \cos \left[ x - \left( l + \frac{1}{2} \right) \frac{\pi}{2} \right], \quad x \gg 1. \quad (8.1-10a)$$

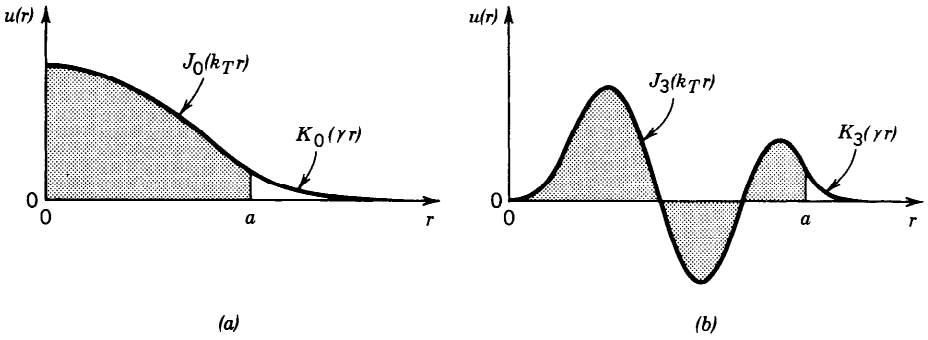


**Figure 8.1-5** Examples of the radial distribution  $u(r)$  given by (8.1-9) for (a)  $l = 0$  and (b)  $l = 3$ . The shaded areas represent the fiber core and the unshaded areas the cladding. The parameters  $k_T$  and  $\gamma$  and the two proportionality constants in (8.1-9) have been selected such that  $u(r)$  is continuous and has a continuous derivative at  $r = a$ . Larger values of  $k_T$  and  $\gamma$  lead to a greater number of oscillations in  $u(r)$ .

In the same limit,  $K_l(x)$  decays with increasing  $x$  at an exponential rate,

$$K_l(x) \approx \left(\frac{\pi}{2x}\right)^{1/2} \left(1 + \frac{4l^2 - 1}{8x}\right) \exp(-x), \quad x \gg 1. \quad (8.1-10b)$$

Two examples of the radial distribution  $u(r)$  are shown in Fig. 8.1-5.

The parameters  $k_T$  and  $\gamma$  determine the rate of change of  $u(r)$  in the core and in the cladding, respectively. A large value of  $k_T$  means faster oscillation of the radial distribution in the core. A large value of  $\gamma$  means faster decay and smaller penetration of the wave into the cladding. As can be seen from (8.1-7), the sum of the squares of  $k_T$  and  $\gamma$  is a constant,

$$k_T^2 + \gamma^2 = (n_1^2 - n_2^2)k_o^2 = NA^2 \cdot k_o^2, \quad (8.1-11)$$

so that as  $k_T$  increases,  $\gamma$  decreases and the field penetrates deeper into the cladding. As  $k_T$  exceeds  $NA \cdot k_o$ ,  $\gamma$  becomes imaginary and the wave ceases to be bound to the core.

**The V Parameter**

It is convenient to normalize  $k_T$  and  $\gamma$  by defining

$$X = k_T a, \quad Y = \gamma a. \quad (8.1-12)$$

In view of (8.1-11),

$$X^2 + Y^2 = V^2, \quad (8.1-13)$$

where  $V = NA \cdot k_o a$ , from which

$$V = 2\pi \frac{a}{\lambda_o} NA.$$

(8.1-14)  
V Parameter

As we shall see shortly,  $V$  is an important parameter that governs the number of modes

of the fiber and their propagation constants. It is called the **fiber parameter** or **V parameter**. It is important to remember that for the wave to be guided,  $X$  must be smaller than  $V$ .

**Modes**

We now consider the boundary conditions. We begin by writing the axial components of the electric- and magnetic-field complex amplitudes  $E_z$  and  $H_z$  in the form of (8.1-5). The condition that these components must be continuous at the core-cladding boundary  $r = a$  establishes a relation between the coefficients of proportionality in (8.1-9), so that we have only one unknown for  $E_z$  and one unknown for  $H_z$ . With the help of Maxwell’s equations,  $j\omega\epsilon_0 n^2 \mathbf{E} = \nabla \times \mathbf{H}$  and  $-j\omega\mu_0 \mathbf{H} = \nabla \times \mathbf{E}$ , the remaining four components  $E_\phi$ ,  $H_\phi$ ,  $E_r$ , and  $H_r$  are determined in terms of  $E_z$  and  $H_z$ . Continuity of  $E_\phi$  and  $H_\phi$  at  $r = a$  yields two more equations. One equation relates the two unknown coefficients of proportionality in  $E_z$  and  $H_z$ ; the other equation gives a condition that the propagation constant  $\beta$  must satisfy. This condition, called the **characteristic equation** or **dispersion relation**, is an equation for  $\beta$  with the ratio  $a/\lambda_0$  and the fiber indices  $n_1, n_2$  as known parameters.

For each azimuthal index  $l$ , the characteristic equation has multiple solutions yielding discrete propagation constants  $\beta_{lm}$ ,  $m = 1, 2, \dots$ , each solution representing a mode. The corresponding values of  $k_T$  and  $\gamma$ , which govern the spatial distributions in the core and in the cladding, respectively, are determined by use of (8.1-7) and are denoted  $k_{Tlm}$  and  $\gamma_{lm}$ . A mode is therefore described by the indices  $l$  and  $m$  characterizing its azimuthal and radial distributions, respectively. The function  $u(r)$  depends on both  $l$  and  $m$ ;  $l = 0$  corresponds to meridional rays. There are two independent configurations of the  $\mathbf{E}$  and  $\mathbf{H}$  vectors for each mode, corresponding to two states of polarization. The classification and labeling of these configurations are generally quite involved (see specialized books in the reading list for more details).

**Characteristic Equation for the Weakly Guiding Fiber**

Most fibers are weakly guiding (i.e.,  $n_1 \approx n_2$  or  $\Delta \ll 1$ ) so that the guided rays are paraxial (i.e., approximately parallel to the fiber axis). The longitudinal components of the electric and magnetic fields are then much weaker than the transverse components and the guided waves are approximately transverse electromagnetic (TEM). The linear polarization in the  $x$  and  $y$  directions then form orthogonal states of polarization. The linearly polarized ( $l, m$ ) mode is usually denoted as the  $LP_{lm}$  mode. The two polarizations of mode ( $l, m$ ) travel with the same propagation constant and have the same spatial distribution.

For weakly guiding fibers the characteristic equation obtained using the procedure outlined earlier turns out to be approximately equivalent to the conditions that the scalar function  $u(r)$  in (8.1-9) is continuous and has a continuous derivative at  $r = a$ . These two conditions are satisfied if

$$\frac{(k_T a) J_l'(k_T a)}{J_l(k_T a)} = \frac{(\gamma a) K_l'(\gamma a)}{K_l(\gamma a)}. \tag{8.1-15}$$

The derivatives  $J_l'$  and  $K_l'$  of the Bessel functions satisfy the identities

$$J_l'(x) = \pm J_{l\mp 1}(x) \mp l \frac{J_l(x)}{x}$$

$$K_l'(x) = -K_{l\mp 1}(x) \mp l \frac{K_l(x)}{x}.$$

Substituting these identities into (8.1-15) and using the normalized parameters  $X = k_T a$  and  $Y = \gamma a$ , we obtain the characteristic equation

$$\boxed{X \frac{J_{l \pm 1}(X)}{J_l(X)} = \pm Y \frac{K_{l \pm 1}(Y)}{K_l(Y)}} \tag{8.1-16}$$

Characteristic Equation

$$\boxed{X^2 + Y^2 = V^2}$$

Given  $V$  and  $l$ , the characteristic equation contains a single unknown variable  $X$  (since  $Y^2 = V^2 - X^2$ ). Note that  $J_{-l}(x) = (-1)^l J_l(x)$  and  $K_{-l}(x) = K_l(x)$ , so that if  $l$  is replaced with  $-l$ , the equation remains unchanged.

The characteristic equation may be solved graphically by plotting its right- and left-hand sides (RHS and LHS) versus  $X$  and finding the intersections. As illustrated in Fig. 8.1-6 for  $l = 0$ , the LHS has multiple branches and the RHS drops monotonically with increase of  $X$  until it vanishes at  $X = V$  ( $Y = 0$ ). There are therefore multiple intersections in the interval  $0 < X \leq V$ . Each intersection point corresponds to a fiber mode with a distinct value of  $X$ . These values are denoted  $X_{lm}$ ,  $m = 1, 2, \dots, M_l$  in order of increasing  $X$ . Once the  $X_{lm}$  are found, the corresponding transverse propagation constants  $k_{Tlm}$ , the decay parameters  $\gamma_{lm}$ , the propagation constants  $\beta_{lm}$ , and the radial distribution functions  $u_{lm}(r)$  may be readily determined by use of (8.1-12), (8.1-7), and (8.1-9). The graph in Fig. 8.1-6 is similar to that in Fig. 7.2-2, which governs the modes of a planar dielectric waveguide.

Each mode has a distinct radial distribution. The radial distributions  $u(r)$  shown in Fig. 8.1-5, for example, correspond to the  $LP_{01}$  mode ( $l = 0, m = 1$ ) in a fiber with  $V = 5$ ; and the  $LP_{34}$  mode ( $l = 3, m = 4$ ) in a fiber with  $V = 25$ . Since the  $(l, m)$  and  $(-l, m)$  modes have the same propagation constant, it is interesting to examine the spatial distribution of their superposition (with equal weights). The complex amplitude of the sum is proportional to  $u_{lm}(r) \cos l\phi \exp(-j\beta_{lm}z)$ . The intensity, which is proportional to  $u_{lm}^2(r) \cos^2 l\phi$ , is illustrated in Fig. 8.1-7 for the  $LP_{01}$  and  $LP_{34}$  modes (the same modes for which  $u(r)$  is shown in Fig. 8.1-5).

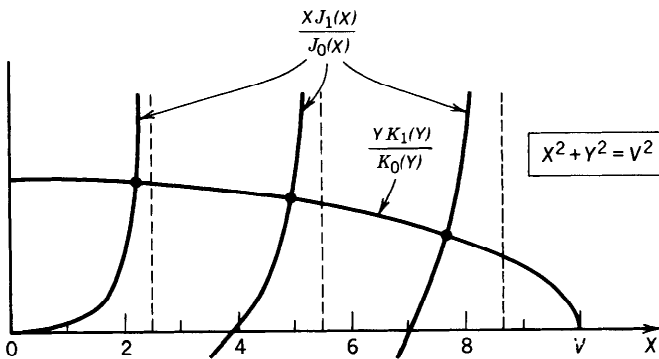


**Figure 8.1-6** Graphical construction for solving the characteristic equation (8.1-16). The left- and right-hand sides are plotted as functions of  $X$ . The intersection points are the solutions. The LHS has multiple branches intersecting the abscissa at the roots of  $J_{l \pm 1}(X)$ . The RHS intersects each branch once and meets the abscissa at  $X = V$ . The number of modes therefore equals the number of roots of  $J_{l \pm 1}(X)$  that are smaller than  $V$ . In this plot  $l = 0$ ,  $V = 10$ , and either the  $-$  or  $+$  signs in (8.1-16) may be taken.

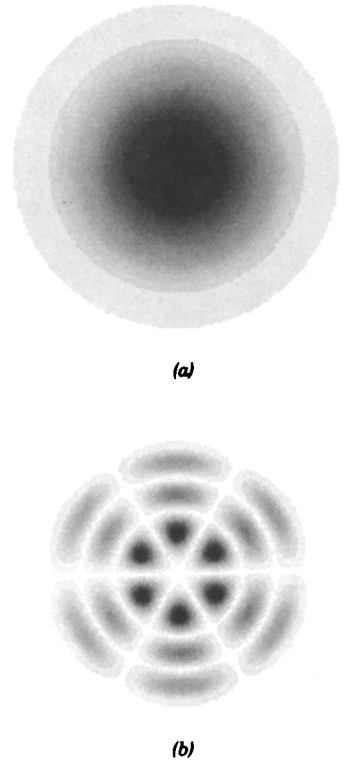


**Figure 8.1-7** Distributions of the intensity of the (a)  $LP_{01}$  and (b)  $LP_{34}$  modes in the transverse plane, assuming an azimuthal  $\cos l\phi$  dependence. The fundamental  $LP_{01}$  mode has a distribution similar to that of the Gaussian beam discussed in Chap. 3.

**Mode Cutoff and Number of Modes**

It is evident from the graphical construction in Fig. 8.1-6 that as  $V$  increases, the number of intersections (modes) increases since the LHS of the characteristic equation (8.1-16) is independent of  $V$ , whereas the RHS moves to the right as  $V$  increases. Considering the minus signs in the characteristic equation, branches of the LHS intersect the abscissa when  $J_{l-1}(X) = 0$ . These roots are denoted by  $x_{lm}$ ,  $m = 1, 2, \dots$ . The number of modes  $M_l$  is therefore equal to the number of roots of  $J_{l-1}(X)$  that are smaller than  $V$ . The  $(l, m)$  mode is allowed if  $V > x_{lm}$ . The mode reaches its cutoff point when  $V = x_{lm}$ . As  $V$  decreases further, the  $(l, m - 1)$  mode also reaches its cutoff point when a new root is reached, and so on. The smallest root of  $J_{l-1}(X)$  is  $x_{01} = 0$  for  $l = 0$  and the next smallest is  $x_{11} = 2.405$  for  $l = 1$ . When  $V < 2.405$ , all modes with the exception of the fundamental  $LP_{01}$  mode are cut off. The fiber then operates as a single-mode waveguide. A plot of the number of modes  $M_l$  as a function of  $V$  is therefore a staircase function increasing by unity at each of the roots  $x_{lm}$  of the Bessel function  $J_{l-1}(X)$ . Some of these roots are listed in Table 8.1-1.

**TABLE 8.1-1 Cutoff  $V$  Parameter for the  $LP_{0m}$  and  $LP_{1m}$  Modes<sup>a</sup>**

$l$	$m$ :	1	2	3
0		0	3.832	7.016
1		2.405	5.520	8.654

<sup>a</sup>The cutoffs of the  $l = 0$  modes occur at the roots of  $J_{-1}(X) = -J_1(X)$ . The  $l = 1$  modes are cut off at the roots of  $J_0(X)$ , and so on.

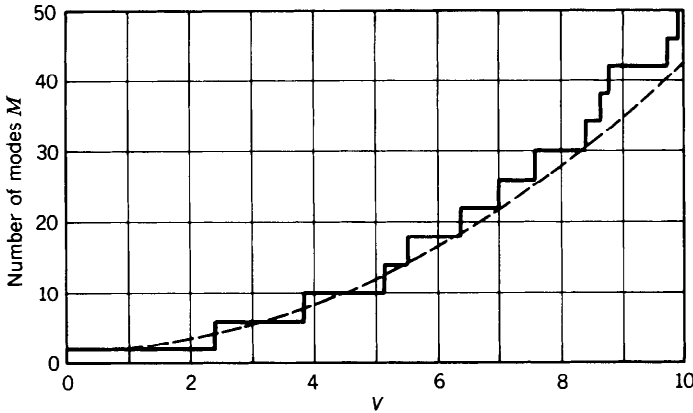


**Figure 8.1-8** Total number of modes  $M$  versus the fiber parameter  $V = 2\pi(a/\lambda_0)NA$ . Included in the count are two helical polarities for each mode with  $l > 0$  and two polarizations per mode. For  $V < 2.405$ , there is only one mode, the fundamental  $LP_{01}$  mode with two polarizations. The dashed curve is the relation  $M = 4V^2/\pi^2 + 2$ , which provides an approximate formula for the number of modes when  $V \gg 1$ .

A composite count of the total number of modes  $M$  (for all  $l$ ) is shown in Fig. 8.1-8 as a function of  $V$ . This is a staircase function with jumps at the roots of  $J_{l-1}(x)$ . Each root must be counted twice since for each mode of azimuthal index  $l > 0$  there is a corresponding mode  $-l$  that is identical except for an opposite polarity of the angle  $\phi$  (corresponding to rays with helical trajectories of opposite senses) as can be seen by using the plus signs in the characteristic equation. In addition, each mode has two states of polarization and must therefore be counted twice.

**Number of Modes (Fibers with Large  $V$  Parameter)**

For fibers with large  $V$  parameters, there are a large number of roots of  $J_l(X)$  in the interval  $0 < X < V$ . Since  $J_l(X)$  is approximated by the sinusoidal function in (8.1-10a) when  $X \gg 1$ , its roots  $x_{lm}$  are approximately given by  $x_{lm} - (l + \frac{1}{2})(\pi/2) = (2m - 1)(\pi/2)$ , i.e.,  $x_{lm} = (l + 2m - \frac{1}{2})\pi/2$ , so that the cutoff points of modes  $(l, m)$ , which are the roots of  $J_{l \pm 1}(X)$ , are

$$x_{lm} \approx \left( l + 2m - \frac{1}{2} \pm 1 \right) \frac{\pi}{2} \approx (l + 2m) \frac{\pi}{2}, \quad l = 0, 1, \dots; \quad m \gg 1, \quad (8.1-17)$$

when  $m$  is large.

For a fixed  $l$ , these roots are spaced uniformly at a distance  $\pi$ , so that the number of roots  $M_l$  satisfies  $(l + 2M_l)\pi/2 = V$ , from which  $M_l \approx V/\pi - l/2$ . Thus  $M_l$  drops linearly with increasing  $l$ , beginning with  $M_l \approx V/\pi$  for  $l = 0$  and ending at  $M_l = 0$  when  $l = l_{max}$ , where  $l_{max} = 2V/\pi$ , as illustrated in Fig. 8.1-9. Thus the total number of modes is  $M \approx \sum_{l=0}^{l_{max}} M_l = \sum_{l=0}^{l_{max}} (V/\pi - l/2)$ .

Since the number of terms in this sum is assumed large, it may be readily evaluated by approximating it as the area of the triangle in Fig. 8.1-9,  $M \approx \frac{1}{2}(2V/\pi)(V/\pi) = V^2/\pi^2$ . Allowing for two degrees of freedom for positive and negative  $l$  and two polarizations for each index  $(l, m)$ , we obtain

$$M \approx \frac{4}{\pi^2} V^2.$$

(8.1-18)  
Number of Modes  
( $V \gg 1$ )

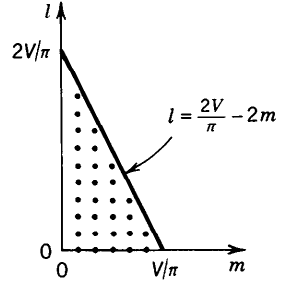


**Figure 8.1-9** The indices of guided modes extend from  $m = 1$  to  $m \approx V/\pi - l/2$  and from  $l = 0$  to  $\approx 2V/\pi$ .

This expression for  $M$  is analogous to that for the rectangular waveguide (7.3-3). Note that (8.1-18) is valid only for large  $V$ . This approximate number is compared to the exact number obtained from the characteristic equation in Fig. 8.1-8.

**EXAMPLE 8.1-2. Approximate Number of Modes.** A silica fiber with  $n_1 = 1.452$  and  $\Delta = 0.01$  has a numerical aperture  $NA = (n_1^2 - n_2^2)^{1/2} \approx n_1(2\Delta)^{1/2} \approx 0.205$ . If  $\lambda_o = 0.85 \mu\text{m}$  and the core radius  $a = 25 \mu\text{m}$ , the  $V$  parameter is  $V = 2\pi(a/\lambda_o)NA \approx 37.9$ . There are therefore approximately  $M \approx 4V^2/\pi^2 \approx 585$  modes. If the cladding is stripped away so that the core is in direct contact with air,  $n_2 = 1$  and  $NA = 1$ . The  $V$  parameter is then  $V = 184.8$  and more than 13,800 modes are allowed.

**Propagation Constants (Fibers with Large  $V$  Parameter)**

As mentioned earlier, the propagation constants can be determined by solving the characteristic equation (8.1-16) for the  $X_{lm}$  and using (8.1-7a) and (8.1-12) to obtain  $\beta_{lm} = (n_1^2 k_o^2 - X_{lm}^2/a^2)^{1/2}$ . A number of approximate formulas for  $X_{lm}$  applicable in certain limits are available in the literature, but there are no explicit exact formulas.

If  $V \gg 1$ , the crudest approximation is to assume that the  $X_{lm}$  are equal to the cutoff values  $x_{lm}$ . This is equivalent to assuming that the branches in Fig. 8.1-6 are approximately vertical lines, so that  $X_{lm} \approx x_{lm}$ . Since  $V \gg 1$ , the majority of the roots would be large and the approximation in (8.1-17) may be used to obtain

$$\beta_{lm} \approx \left[ n_1^2 k_o^2 - (l + 2m)^2 \frac{\pi^2}{4a^2} \right]^{1/2} \tag{8.1-19}$$

Since

$$M \approx \frac{4}{\pi^2} V^2 = \frac{4}{\pi^2} NA^2 \cdot a^2 k_o^2 \approx \frac{4}{\pi^2} (2n_1^2 \Delta) k_o^2 a^2, \tag{8.1-20}$$

(8.1-19) and (8.1-20) give

$$\beta_{lm} \approx n_1 k_o \left[ 1 - 2 \frac{(l + 2m)^2}{M} \Delta \right]^{1/2} \tag{8.1-21}$$

Because  $\Delta$  is small we use the approximation  $(1 + \delta)^{1/2} \approx 1 + \delta/2$  for  $|\delta| \ll 1$ , and

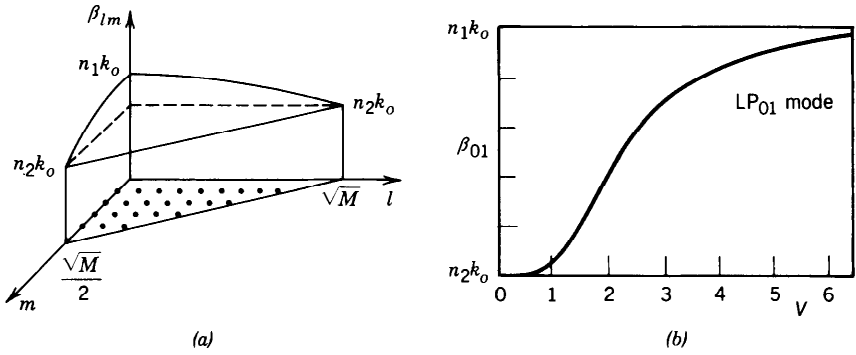


**Figure 8.1-10** (a) Approximate propagation constants  $\beta_{lm}$  of the modes of a fiber with large  $V$  parameter as functions of the mode indices  $l$  and  $m$ . (b) Exact propagation constant  $\beta_{01}$  of the fundamental  $LP_{01}$  modes as a function of the  $V$  parameter. For  $V \gg 1$ ,  $\beta_{01} \approx n_1 k_o$ .

obtain

$$\beta_{lm} \approx n_1 k_o \left[ 1 - \frac{(l + 2m)^2}{M} \Delta \right]. \tag{8.1-22}$$

Propagation Constants  
 $l = 0, 1, \dots, \sqrt{M}$   
 $m = 1, 2, \dots, (\sqrt{M} - l)/2$   
 $(V \gg 1)$

Since  $l + 2m$  varies between 2 and  $\approx 2V/\pi = \sqrt{M}$  (see Fig. 8.1-9),  $\beta_{lm}$  varies approximately between  $n_1 k_o$  and  $n_1 k_o(1 - \Delta) \approx n_2 k_o$ , as illustrated in Fig. 8.1-10.

**Group Velocities (Fibers with Large  $V$  Parameter)**

To determine the group velocity,  $v_{lm} = d\omega/d\beta_{lm}$ , of the  $(l, m)$  mode we express  $\beta_{lm}$  as an explicit function of  $\omega$  by substituting  $n_1 k_o = \omega/c_1$  and  $M = (4/\pi^2)(2n_1^2 \Delta)k_o^2 a^2 = (8/\pi^2)a^2 \omega^2 \Delta/c_1^2$  into (8.1-22) and assume that  $c_1$  and  $\Delta$  are independent of  $\omega$ . The derivative  $d\omega/d\beta_{lm}$  gives

$$v_{lm} \approx c_1 \left[ 1 + \frac{(l + 2m)^2}{M} \Delta \right]^{-1}.$$

Since  $\Delta \ll 1$ , the approximate expansion  $(1 + \delta)^{-1} \approx 1 - \delta$  when  $|\delta| \ll 1$ , gives

$$v_{lm} \approx c_1 \left[ 1 - \frac{(l + 2m)^2}{M} \Delta \right]. \tag{8.1-23}$$

Group Velocities  
 $(V \gg 1)$

Because the minimum and maximum values of  $(l + 2m)$  are 2 and  $\sqrt{M}$ , respectively, and since  $M \gg 1$ , the group velocity varies approximately between  $c_1$  and  $c_1(1 - \Delta) = c_1(n_2/n_1)$ . Thus the group velocities of the low-order modes are approximately equal to the phase velocity of the core material, and those of the high-order modes are smaller.

The fractional group-velocity change between the fastest and the slowest mode is roughly equal to  $\Delta$ , the fractional refractive index change of the fiber. Fibers with large  $\Delta$ , although endowed with a large NA and therefore large light-gathering capacity, also have a large number of modes, large modal dispersion, and consequently high pulse spreading rates. These effects are particularly severe if the cladding is removed altogether.

### C. Single-Mode Fibers

As discussed earlier, a fiber with core radius  $a$  and numerical aperture NA operates as a single-mode fiber in the fundamental  $LP_{01}$  mode if  $V = 2\pi(a/\lambda_o)NA < 2.405$  (see Table 8.1-1 on page 282). Single-mode operation is therefore achieved by using a small core diameter and small numerical aperture (making  $n_2$  close to  $n_1$ ), or by operating at a sufficiently long wavelength. The fundamental mode has a bell-shaped spatial distribution similar to the Gaussian distribution [see Figs. 8.1-5(a) and 8.1-7(a)] and a propagation constant  $\beta$  that depends on  $V$  as illustrated in Fig. 8.1-10(b). This mode provides the highest confinement of light power within the core.

---

**EXAMPLE 8.1-3. Single-Mode Operation.** A silica glass fiber with  $n_1 = 1.447$  and  $\Delta = 0.01$  (NA = 0.205) operates at  $\lambda_o = 1.3 \mu\text{m}$  as a single-mode fiber if  $V = 2\pi(a/\lambda_o)NA < 2.405$ , i.e., if the core diameter  $2a < 4.86 \mu\text{m}$ . If  $\Delta$  is reduced to 0.0025, single-mode operation requires a diameter  $2a < 9.72 \mu\text{m}$ .

---

There are numerous advantages of using single-mode fibers in optical communication systems. As explained earlier, the modes of a multimode fiber travel at different group velocities and therefore undergo different time delays, so that a short-duration pulse of multimode light is delayed by different amounts and therefore spreads in time. Quantitative measures of modal dispersion are determined in Sec. 8.3B. In a single-mode fiber, on the other hand, there is only one mode with one group velocity, so that a short pulse of light arrives without delay distortion. As explained in Sec. 8.3B, other dispersion effects result in pulse spreading in single-mode fibers, but these are significantly smaller than modal dispersion.

As also shown in Sec. 8.3, the rate of power attenuation is lower in a single-mode fiber than in a multimode fiber. This, together with the smaller pulse spreading rate, permits substantially higher data rates to be transmitted by single-mode fibers in comparison with the maximum rates feasible with multimode fibers. This topic is discussed in Chap. 22.

Another difficulty with multimode fibers is caused by the random interference of the modes. As a result of uncontrollable imperfections, strains, and temperature fluctuations, each mode undergoes a random phase shift so that the sum of the complex amplitudes of the modes has a random intensity. This randomness is a form of noise known as **modal noise** or **speckle**. This effect is similar to the fading of radio signals due to multiple-path transmission. In a single-mode fiber there is only one path and therefore no modal noise.

Because of their small size and small numerical apertures, single-mode fibers are more compatible with integrated-optics technology. However, such features make them more difficult to manufacture and work with because of the reduced allowable mechanical tolerances for splicing or joining with demountable connectors and for coupling optical power into the fiber.

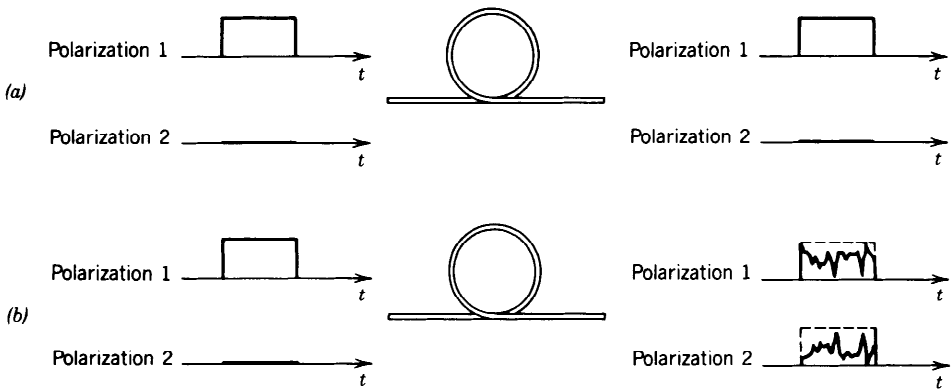


**Figure 8.1-11** (a) Ideal polarization-maintaining fiber. (b) Random transfer of power between two polarizations.

### Polarization-Maintaining Fibers

In a fiber with circular cross section, each mode has two independent states of polarization with the same propagation constant. Thus the fundamental  $LP_{01}$  mode in a single-mode weakly guiding fiber may be polarized in the  $x$  or  $y$  direction with the two orthogonal polarizations having the same propagation constant and the same group velocity.

In principle, there is no exchange of power between the two polarization components. If the power of the light source is delivered into one polarization only, the power received remains in that polarization. In practice, however, slight random imperfections or uncontrollable strains in the fiber result in random power transfer between the two polarizations. This coupling is facilitated since the two polarizations have the same propagation constant and their phases are therefore matched. Thus linearly polarized light at the fiber input is transformed into elliptically polarized light at the output. As a result of fluctuations of strain, temperature, or source wavelength, the ellipticity of the received light fluctuates randomly with time. Nevertheless, the total power remains fixed (Fig. 8.1-11). If we are interested only in transmitting light power, this randomization of the power division between the two polarization components poses no difficulty, provided that the total power is collected.

In many areas related to fiber optics, e.g., coherent optical communications, integrated-optic devices, and optical sensors based on interferometric techniques, the fiber is used to transmit the complex amplitude of a specific polarization (magnitude and phase). For these applications, polarization-maintaining fibers are necessary. To make a polarization-maintaining fiber the circular symmetry of the conventional fiber must be removed, by using fibers with elliptical cross sections or stress-induced anisotropy of the refractive index, for example. This eliminates the polarization degeneracy, i.e., makes the propagation constants of the two polarizations different. The coupling efficiency is then reduced as a result of the introduction of phase mismatch.

## 8.2 GRADED-INDEX FIBERS

Index grading is an ingenious method for reducing the pulse spreading caused by the differences in the group velocities of the modes of a multimode fiber. The core of a graded-index fiber has a varying refractive index, highest in the center and decreasing gradually to its lowest value at the cladding. The phase velocity of light is therefore minimum at the center and increases gradually with the radial distance. Rays of the

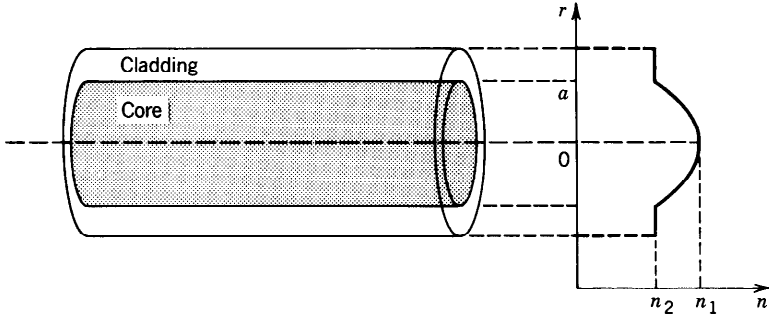


**Figure 8.2-1** Geometry and refractive-index profile of a graded-index fiber.

most axial mode travel the shortest distance at the smallest phase velocity. Rays of the most oblique mode zigzag at a greater angle and travel a longer distance, mostly in a medium where the phase velocity is high. Thus the disparities in distances are compensated by opposite disparities in phase velocities. As a consequence, the differences in the group velocities and the travel times are expected to be reduced. In this section we examine the propagation of light in graded-index fibers.

The core refractive index is a function  $n(r)$  of the radial position  $r$  and the cladding refractive index is a constant  $n_2$ . The highest value of  $n(r)$  is  $n(0) = n_1$  and the lowest value occurs at the core radius  $r = a$ ,  $n(a) = n_2$ , as illustrated in Fig. 8.2-1.

A versatile refractive-index profile is the power-law function

$$n^2(r) = n_1^2 \left[ 1 - 2 \left( \frac{r}{a} \right)^p \Delta \right], \quad r \leq a, \tag{8.2-1}$$

where

$$\Delta = \frac{n_1^2 - n_2^2}{2n_1^2} \approx \frac{n_1 - n_2}{n_1}, \tag{8.2-2}$$

and  $p$ , called the **grade profile parameter**, determines the steepness of the profile. This function drops from  $n_1$  at  $r = 0$  to  $n_2$  at  $r = a$ . For  $p = 1$ ,  $n^2(r)$  is linear, and for  $p = 2$  it is quadratic. As  $p \rightarrow \infty$ ,  $n^2(r)$  approaches a step function, as illustrated in Fig. 8.2-2. Thus the step-index fiber is a special case of the graded-index fiber with  $p = \infty$ .

**Guided Rays**

The transmission of light rays in a graded-index medium with parabolic-index profile was discussed in Sec. 1.3. Rays in meridional planes follow oscillatory planar trajecto-

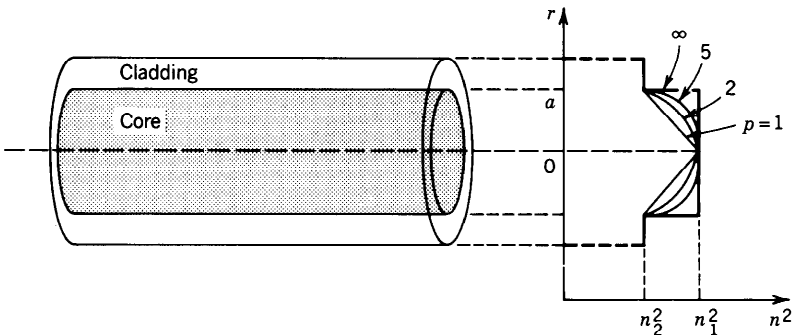


**Figure 8.2-2** Power-law refractive-index profile  $n^2(r)$  for different values of  $p$ .

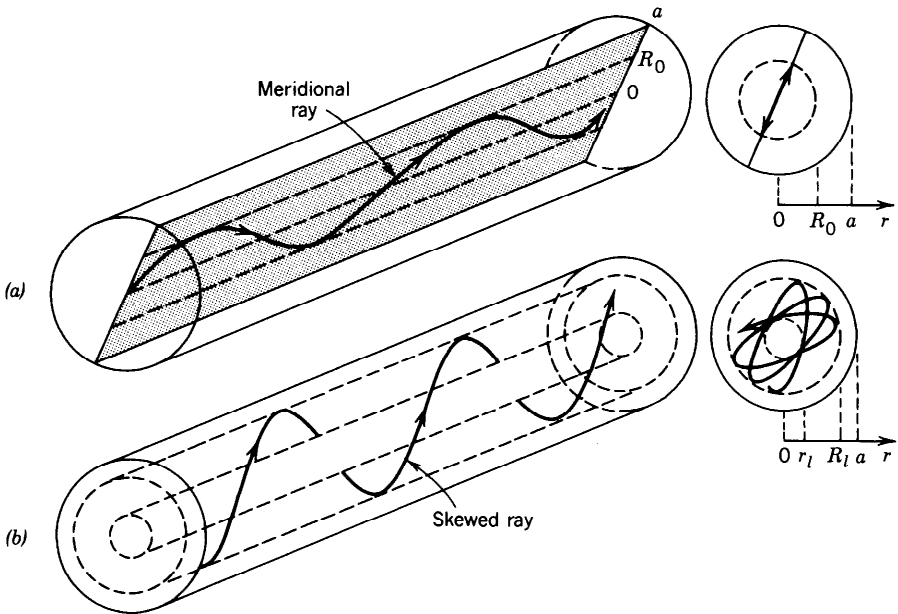


**Figure 8.2-3** Guided rays in the core of a graded-index fiber. (a) A meridional ray confined to a meridional plane inside a cylinder of radius  $R_0$ . (b) A skewed ray follows a helical trajectory confined within two cylindrical shells of radii  $r_1$  and  $R_1$ .

ries, whereas skewed rays follow helical trajectories with the turning points forming cylindrical caustic surfaces, as illustrated in Fig. 8.2-3. Guided rays are confined within the core and do not reach the cladding.

## A. Guided Waves

The modes of the graded-index fiber may be determined by writing the Helmholtz equation (8.1-4) with  $n = n(r)$ , solving for the spatial distributions of the field components, and using Maxwell's equations and the boundary conditions to obtain the characteristic equation as was done in the step-index case. This procedure is in general difficult.

In this section we use instead an approximate approach based on picturing the field distribution as a quasi-plane wave traveling within the core, approximately along the trajectory of the optical ray. A quasi-plane wave is a wave that is locally identical to a plane wave, but changes its direction and amplitude slowly as it travels. This approach permits us to maintain the simplicity of rays optics but retain the phase associated with the wave, so that we can use the self-consistency condition to determine the propagation constants of the guided modes (as was done in the planar waveguide in Sec. 7.2). This approximate technique, called the WKB (Wentzel-Kramers-Brillouin) method, is applicable only to fibers with a large number of modes (large  $V$  parameter).

### Quasi-Plane Waves

Consider a solution of the Helmholtz equation (8.1-4) in the form of a quasi-plane wave (see Sec. 2.3)

$$U(\mathbf{r}) = a(\mathbf{r}) \exp[-jk_o S(\mathbf{r})], \quad (8.2-3)$$

where  $a(\mathbf{r})$  and  $S(\mathbf{r})$  are real functions of position that are slowly varying in comparison with the wavelength  $\lambda_o = 2\pi/k_o$ . We know from Sec. 2.3 that  $S(\mathbf{r})$  approximately

satisfies the eikonal equation  $|\nabla S|^2 \approx n^2$ , and that the rays travel in the direction of the gradient  $\nabla S$ . If we take  $k_o S(\mathbf{r}) = k_o s(r) + l\phi + \beta z$ , where  $s(r)$  is a slowly varying function of  $r$ , the eikonal equation gives

$$\left(k_o \frac{ds}{dr}\right)^2 + \beta^2 + \frac{l^2}{r^2} = n^2(r)k_o^2. \tag{8.2-4}$$

The local spatial frequency of the wave in the radial direction is the partial derivative of the phase  $k_o S(\mathbf{r})$  with respect to  $r$ ,

$$k_r = k_o \frac{ds}{dr}, \tag{8.2-5}$$

so that (8.2-3) becomes

$$U(r) = a(r) \exp\left(-j \int_0^r k_r dr\right) e^{-jl\phi} e^{-j\beta z}, \tag{8.2-6}$$

Quasi-Plane Wave

and (8.2-4) gives

$$k_r^2 = n^2(r)k_o^2 - \beta^2 - \frac{l^2}{r^2}. \tag{8.2-7}$$

Defining  $k_\phi = l/r$ , i.e.,  $\exp(-jl\phi) = \exp(-jk_\phi r\phi)$ , and  $k_z = \beta$ , we find that (8.2-7) gives  $k_r^2 + k_\phi^2 + k_z^2 = n^2(r)k_o^2$ . The quasi-plane wave therefore has a local wavevector  $\mathbf{k}$  with magnitude  $n(r)k_o$  and cylindrical-coordinate components  $(k_r, k_\phi, k_z)$ . Since  $n(r)$  and  $k_\phi$  are functions of  $r$ ,  $k_r$  is also generally position dependent. The direction of  $\mathbf{k}$  changes slowly with  $r$  (see Fig. 8.2-4) following a helical trajectory similar to that of the skewed ray shown earlier in Fig. 8.2-3(b).

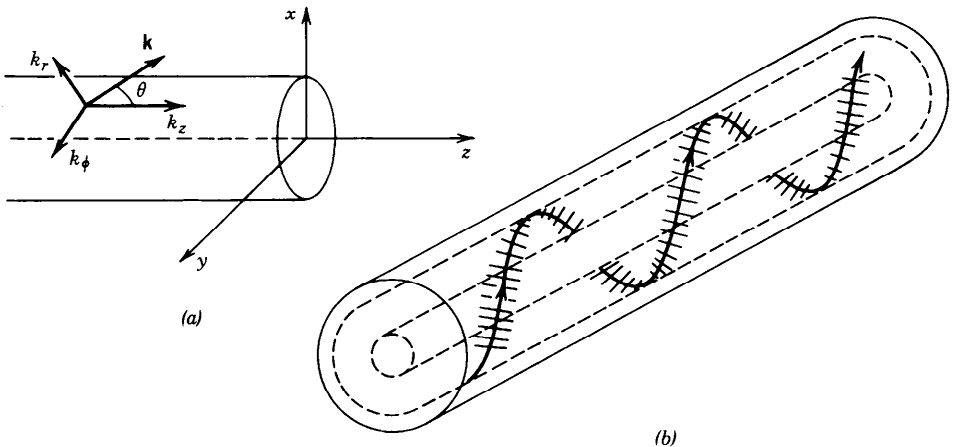


**Figure 8.2-4** (a) The wavevector  $\mathbf{k} = (k_r, k_\phi, k_z)$  in a cylindrical coordinate system. (b) Quasi-plane wave following the direction of a ray.

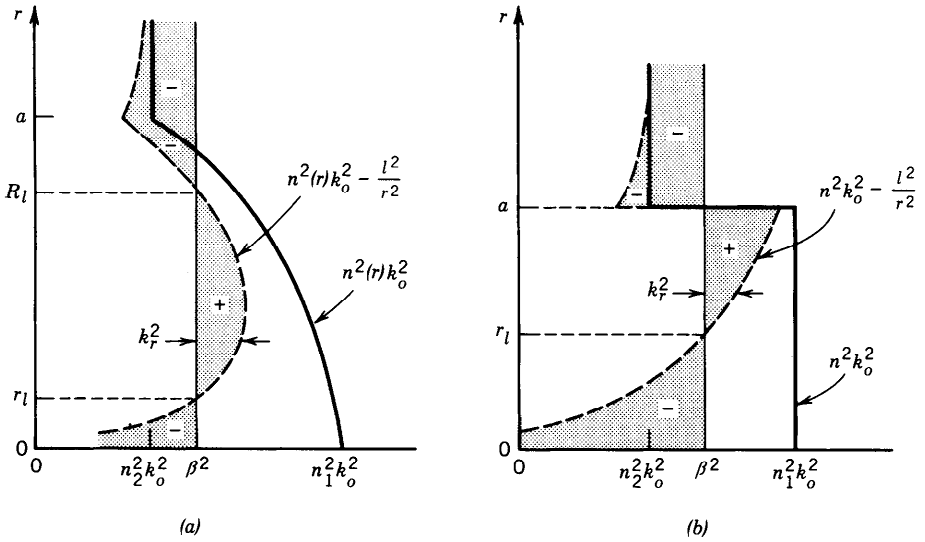


**Figure 8.2-5** Dependence of  $n^2(r)k_o^2$ ,  $n^2(r)k_o^2 - l^2/r^2$ , and  $k_r^2 = n^2(r)k_o^2 - l^2/r^2 - \beta^2$  on the position  $r$ . At any  $r$ ,  $k_r^2$  is the width of the shaded area with the + and - signs denoting positive and negative  $k_r^2$ . (a) Graded-index fiber;  $k_r^2$  is positive in the region  $r_l < r < R_l$ . (b) Step-index fiber;  $k_r^2$  is positive in the region  $r_l < r < a$ .

To determine the region of the core within which the wave is bound, we determine the values of  $r$  for which  $k_r$  is real, or  $k_r^2 > 0$ . For a given  $l$  and  $\beta$  we plot  $k_r^2 = [n^2(r)k_o^2 - l^2/r^2 - \beta^2]$  as a function of  $r$ . The term  $n^2(r)k_o^2$  is first plotted as a function of  $r$  [the thick continuous curve in Fig. 8.2-5(a)]. The term  $l^2/r^2$  is then subtracted, yielding the dashed curve. The value of  $\beta^2$  is marked by the thin continuous vertical line. It follows that  $k_r^2$  is represented by the difference between the dashed line and the thin continuous line, i.e., by the shaded area. Regions where  $k_r^2$  is positive or negative are indicated by the + or - signs, respectively. Thus  $k_r$  is real in the region  $r_l < r < R_l$ , where

$$n^2(r)k_o^2 - \frac{l^2}{r^2} - \beta^2 = 0, \quad r = r_l \quad \text{and} \quad r = R_l. \quad (8.2-8)$$

It follows that the wave is basically confined within a cylindrical shell of radii  $r_l$  and  $R_l$  just like the helical ray trajectory shown in Fig. 8.2-3(b).

These results are also applicable to the step-index fiber in which  $n(r) = n_1$  for  $r < a$ , and  $n(r) = n_2$  for  $r > a$ . In this case the quasi-plane wave is guided in the core by reflecting from the core-cladding boundary at  $r = a$ . As illustrated in Fig. 8.2-5(b), the region of confinement is  $r_l < r < a$ , where

$$n_1^2 k_o^2 - \frac{l^2}{r_l^2} - \beta^2 = 0. \quad (8.2-9)$$

The wave bounces back and forth helically like the skewed ray shown in Fig. 8.1-2. In the cladding ( $r > a$ ) and near the center of the core ( $r < r_l$ ),  $k_r^2$  is negative so that  $k_r$  is imaginary, and the wave therefore decays exponentially. Note that  $r_l$  depends on  $\beta$ . For large  $\beta$  (or large  $l$ ),  $r_l$  is large; i.e., the wave is confined to a thin cylindrical shell near the edge of the core.

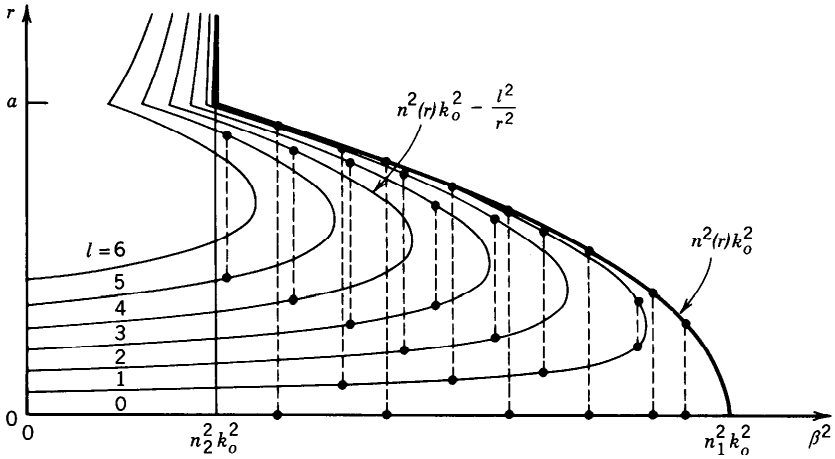


**Figure 8.2-6** The propagation constants and confinement regions of the fiber modes. Each curve corresponds to an index  $l$ . In this plot  $l = 0, 1, \dots, 6$ . Each mode (representing a certain value of  $m$ ) is marked schematically by two dots connected by a dashed vertical line. The ordinates of the dots mark the radii  $r_l$  and  $R_l$  of the cylindrical shell within which the mode is confined. Values on the abscissa are the squared propagation constants  $\beta^2$  of the mode.

**Modes**

The modes of the fiber are determined by imposing the self-consistency condition that the wave reproduce itself after one helical period of traveling between  $r_l$  and  $R_l$  and back. The azimuthal path length corresponding to an angle  $2\pi$  must correspond to a multiple of  $2\pi$  phase shift, i.e.,  $k_\phi 2\pi r = 2\pi l$ ;  $l = 0, \pm 1, \pm 2, \dots$ . This condition is evidently satisfied since  $k_\phi = l/r$ . In addition, the radial round-trip path length must correspond to a phase shift equal to an integer multiple of  $2\pi$ ,

$$2 \int_{r_l}^{R_l} k_r dr = 2\pi m, \quad m = 1, 2, \dots, M_l. \tag{8.2-10}$$

This condition, which is analogous to the self-consistency condition (7.2-2) for planar waveguides, provides the characteristic equation from which the propagation constants  $\beta_{lm}$  of the modes are determined. These values are marked schematically in Fig. 8.2-6; the mode  $m = 1$  has the largest value of  $\beta$  (approximately  $n_1 k_o$ ) and  $m = M_l$  has the smallest value (approximately  $n_2 k_o$ ).

**Number of Modes**

The total number of modes can be determined by adding the number of modes  $M_l$  for  $l = 0, 1, \dots, l_{\max}$ . We shall address this problem using a different procedure. We first determine the number  $q_\beta$  of modes with propagation constants greater than a given value  $\beta$ . For each  $l$ , the number of modes  $M_l(\beta)$  with propagation constant greater than  $\beta$  is the number of multiples of  $2\pi$  the integral in (8.2-10) yields, i.e.,

$$M_l(\beta) = \frac{1}{\pi} \int_{r_l}^{R_l} k_r dr = \frac{1}{\pi} \int_{r_l}^{R_l} \left[ n^2(r)k_o^2 - \frac{l^2}{r^2} - \beta^2 \right]^{1/2} dr, \tag{8.2-11}$$

where  $r_l$  and  $R_l$  are the radii of confinement corresponding to the propagation constant  $\beta$  as given by (8.2-8). Clearly,  $r_l$  and  $R_l$  depend on  $\beta$ .

The total number of modes with propagation constant greater than  $\beta$  is therefore

$$q_\beta = 4 \sum_{l=0}^{l_{\max}(\beta)} M_l(\beta), \tag{8.2-12}$$

where  $l_{\max}(\beta)$  is the maximum value of  $l$  that yields a bound mode with propagation constants greater than  $\beta$ , i.e., for which the peak value of the function  $n^2(r)k_o^2 - l^2/r^2$  is greater than  $\beta^2$ . The grand total number of modes  $M$  is  $q_\beta$  for  $\beta = n_2 k_o$ . The factor of 4 in (8.2-12) accounts for the two possible polarizations and the two possible polarities of the angle  $\phi$ , corresponding to positive or negative helical trajectories for each  $(l, m)$ . If the number of modes is sufficiently large, we can replace the summation in (8.2-12) by an integral,

$$q_\beta \approx 4 \int_0^{l_{\max}(\beta)} M_l(\beta) dl. \tag{8.2-13}$$

For fibers with a power-law refractive-index profile, we substitute (8.2-1) into (8.2-11), and the result into (8.2-13), and evaluate the integral to obtain

$$q_\beta \approx M \left[ \frac{1 - (\beta/n_1 k_o)^2}{2\Delta} \right]^{(p+2)/p}, \tag{8.2-14}$$

where

$$M \approx \frac{p}{p+2} n_1^2 k_o^2 a^2 \Delta = \frac{p}{p+2} \frac{V^2}{2}. \tag{8.2-15}$$

Here  $\Delta = (n_1 - n_2)/n_1$  and  $V = 2\pi(a/\lambda_o)NA$  is the fiber  $V$  parameter. Since  $q_\beta \approx M$  at  $\beta = n_2 k_o$ ,  $M$  is indeed the total number of modes.

For step-index fibers ( $p = \infty$ ),

$$q_\beta \approx M \left[ \frac{1 - (\beta/n_1 k_o)^2}{2\Delta} \right] \tag{8.2-16}$$

and

$$M \approx \frac{V^2}{2}. \tag{8.2-17}$$

Number of Modes  
(Step-Index Fiber)  
 $V = 2\pi(a/\lambda_o)NA$

This expression for  $M$  is nearly the same as  $M \approx 4V^2/\pi^2 \approx 0.41V^2$  in (8.1-18), which was obtained in Sec. 8.1 using a different approximation.

### B. Propagation Constants and Velocities

#### Propagation Constants

The propagation constant  $\beta_q$  of mode  $q$  is obtained by inverting (8.2-14),

$$\beta_q \approx n_1 k_o \left[ 1 - 2 \left( \frac{q}{M} \right)^{p/(p+2)} \Delta \right]^{1/2}, \quad q = 1, 2, \dots, M, \quad (8.2-18)$$

where the index  $q_\beta$  has been replaced by  $q$ , and  $\beta$  replaced by  $\beta_q$ . Since  $\Delta \ll 1$ , the approximation  $(1 + \delta)^{1/2} \approx 1 + \frac{1}{2}\delta$  (when  $|\delta| \ll 1$ ) can be applied to (8.2-18), yielding

$$\beta_q \approx n_1 k_o \left[ 1 - \left( \frac{q}{M} \right)^{p/(p+2)} \Delta \right].$$

(8.2-19)  
Propagation Constants  
 $q = 1, 2, \dots, M$

The propagation constant  $\beta_q$  therefore decreases from  $\approx n_1 k_o$  (at  $q = 1$ ) to  $n_2 k_o$  (at  $q = M$ ), as illustrated in Fig. 8.2-7.

In the step-index fiber ( $p = \infty$ ),

$$\beta_q \approx n_1 k_o \left( 1 - \frac{q}{M} \Delta \right).$$

(8.2-20)  
Propagation Constants  
(Step-Index Fiber)  
 $q = 1, 2, \dots, M$

This expression is identical to (8.1-22) if the index  $q = 1, 2, \dots, M$  is replaced by  $(l + 2m)^2$ , where  $l = 0, 1, \dots, \sqrt{M}$ ;  $m = 1, 2, \dots, \sqrt{M}/2 - l/2$ .

#### Group Velocities

To determine the group velocity  $v_g = d\omega/d\beta_q$ , we write  $\beta_q$  as a function of  $\omega$  by substituting (8.2-15) into (8.2-19), substituting  $n_1 k_o = \omega/c_1$  into the result, and evaluating  $v_g = (d\beta_q/d\omega)^{-1}$ . With the help of the approximation  $(1 + \delta)^{-1} \approx 1 - \delta$  when

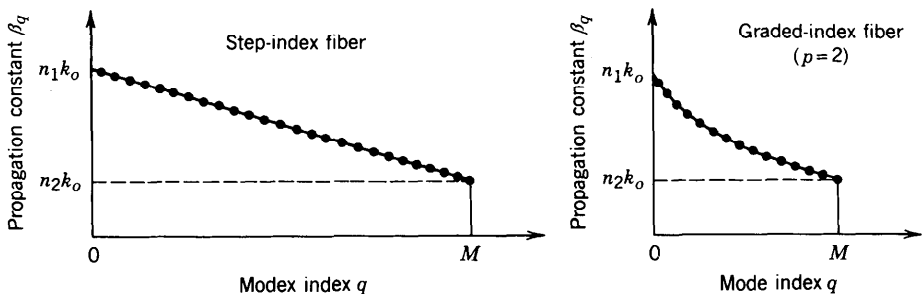


**Figure 8.2-7** Dependence of the propagation constants  $\beta_q$  on the mode index  $q = 1, 2, \dots, M$ .

$|\delta| \ll 1$ , and assuming that  $c_1$  and  $\Delta$  are independent of  $\omega$  (i.e., ignoring material dispersion), we obtain

$$v_q \approx c_1 \left[ 1 - \frac{p-2}{p+2} \left( \frac{q}{M} \right)^{p/(p+2)} \Delta \right]. \tag{8.2-21}$$

Group Velocities  
 $q = 1, 2, \dots, M$

For the step-index fiber ( $p = \infty$ )

$$v_q \approx c_1 \left( 1 - \frac{q}{M} \Delta \right). \tag{8.2-22}$$

Group Velocities  
(Step-Index Fiber)  
 $q = 1, 2, \dots, M$

The group velocity varies from approximately  $c_1$  to  $c_1(1 - \Delta)$ . This reproduces the result obtained in (8.1-23).

**Optimal Index Profile**

Equation (8.2-21) indicates that the grade profile parameter  $p = 2$  yields a group velocity  $v_q \approx c_1$  for all  $q$ , so that all modes travel at approximately the same velocity  $c_1$ . The advantage of the graded-index fiber for multimode transmission is now apparent.

To determine the group velocity with better accuracy, we repeat the derivation of  $v_q$  from (8.2-18), taking three terms in the Taylor's expansion  $(1 + \delta)^{1/2} \approx 1 + \delta/2 - \delta^2/8$ , instead of two. For  $p = 2$ , the result is

$$v_q = c_1 \left( 1 - \frac{q}{M} \frac{\Delta^2}{2} \right). \tag{8.2-23}$$

Group Velocities  
( $p = 2$ )  
 $q = 1, \dots, M$

Thus the group velocities vary from approximately  $c_1$  at  $q = 1$  to approximately  $c_1(1 - \Delta^2/2)$  at  $q = M$ . In comparison with the step-index fiber, for which the group velocity ranges between  $c_1$  and  $c_1(1 - \Delta)$ , the fractional velocity difference for the parabolically graded fiber is  $\Delta^2/2$  instead of  $\Delta$  for the step-index fiber (Fig. 8.2-8). Under ideal conditions, the graded-index fiber therefore reduces the group velocity

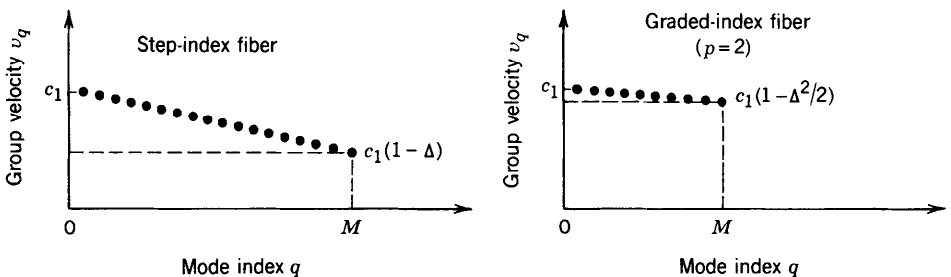


**Figure 8.2-8** Group velocities  $v_q$  of the modes of a step-index fiber ( $p = \infty$ ) and an optimal graded-index fiber ( $p = 2$ ).

difference by a factor  $\Delta/2$ , thus realizing its intended purpose of equalizing the mode velocities. Since the analysis leading to (8.2-23) is based on a number of approximations, however, this improvement factor is only a rough estimate; indeed it is not fully attained in practice.

For  $p = 2$ , the number of modes  $M$  given by (8.2-15) becomes

$$M \approx \frac{V^2}{4} \tag{8.2-24}$$

Number of Modes  
(Graded-Index Fiber,  $p = 2$ )  
 $V = 2\pi(a/\lambda_o)NA$

Comparing this with (8.2-17), we see that the number of modes in an optimal graded-index fiber is approximately one-half the number of modes in a step-index fiber of the same parameters  $n_1, n_2$ , and  $a$ .

### 8.3 ATTENUATION AND DISPERSION

Attenuation and dispersion limit the performance of the optical-fiber medium as a data transmission channel. Attenuation limits the magnitude of the optical power transmitted, whereas dispersion limits the rate at which data may be transmitted through the fiber, since it governs the temporal spreading of the optical pulses carrying the data.

#### A. Attenuation

##### The Attenuation Coefficient

Light traveling through an optical fiber exhibits a power that decreases exponentially with the distance as a result of absorption and scattering. The attenuation coefficient  $\alpha$  is usually defined in units of dB/km,

$$\alpha = \frac{1}{L} 10 \log_{10} \frac{1}{\mathcal{T}}, \tag{8.3-1}$$

where  $\mathcal{T} = P(L)/P(0)$  is the power transmission ratio (ratio of transmitted to incident power) for a fiber of length  $L$  km. The relation between  $\alpha$  and  $\mathcal{T}$  is illustrated in Fig. 8.3-1 for  $L = 1$  km. A 3-dB attenuation, for example, corresponds to  $\mathcal{T} = 0.5$ , while 10 dB is equivalent to  $\mathcal{T} = 0.1$  and 20 dB corresponds to  $\mathcal{T} = 0.01$ , and so on.

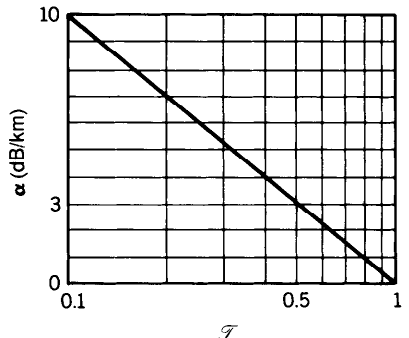


Figure 8.3-1 Relation between transmittance  $\mathcal{T}$  and attenuation coefficient  $\alpha$  in dB units.

Losses in dB units are additive, whereas the transmission ratios are multiplicative. Thus for a propagation distance of  $z$  kilometers, the loss is  $\alpha z$  decibels and the power transmission ratio is

$$\frac{P(z)}{P(0)} = 10^{-\alpha z/10} \approx e^{-0.23\alpha z}. \quad (\alpha \text{ in dB/km}) \quad (8.3-2)$$

Note that if the attenuation coefficient is measured in  $\text{km}^{-1}$  units, instead of in dB/km, then

$$P(z)/P(0) = e^{-\alpha z} \quad (8.3-3)$$

where  $\alpha \approx 0.23\alpha$ . Throughout this section  $\alpha$  is taken in dB/km units so that (8.3-2) applies. Elsewhere in the book, however, we use  $\alpha$  to denote the attenuation coefficient ( $\text{m}^{-1}$  or  $\text{cm}^{-1}$ ) in which case the power attenuation is described by (8.3-3).

### Absorption

The attenuation coefficient of fused silica glass ( $\text{SiO}_2$ ) is strongly dependent on wavelength, as illustrated in Fig. 8.3-2. This material has two strong absorption bands: a middle-infrared absorption band resulting from vibrational transitions and an ultraviolet absorption band due to electronic and molecular transitions. There is a window bounded by the tails of these bands in which there is essentially no intrinsic absorption. This window occupies the near-infrared region.

### Scattering

**Rayleigh scattering** is another intrinsic effect that contributes to the attenuation of light in glass. The random localized variations of the molecular positions in glass create random inhomogeneities of the refractive index that act as tiny scattering centers. The amplitude of the scattered field is proportional to  $\omega^2$ .<sup>†</sup> The scattered intensity is therefore proportional to  $\omega^4$  or to  $1/\lambda_o^4$ , so that short wavelengths are scattered more than long wavelengths. Thus blue light is scattered more than red (a similar effect, the

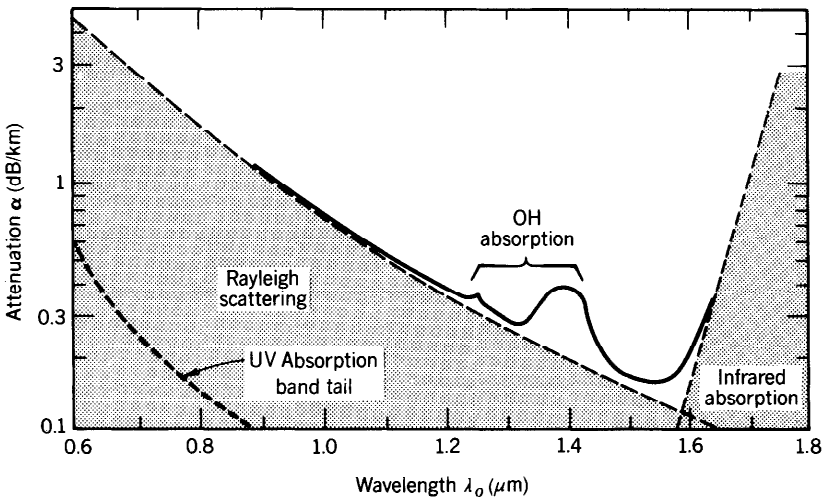


**Figure 8.3-2** Dependence of the attenuation coefficient  $\alpha$  of silica glass on the wavelength  $\lambda_o$ . There is a local minimum at  $1.3 \mu\text{m}$  ( $\alpha \approx 0.3 \text{ dB/km}$ ) and an absolute minimum at  $1.55 \mu\text{m}$  ( $\alpha \approx 0.16 \text{ dB/km}$ ).

<sup>†</sup>The scattering medium creates a polarization density  $\mathcal{P}$  which corresponds to a source of radiation proportional to  $d^2\mathcal{P}/dt^2 = -\omega^2\mathcal{P}$ ; see (5.2-19).

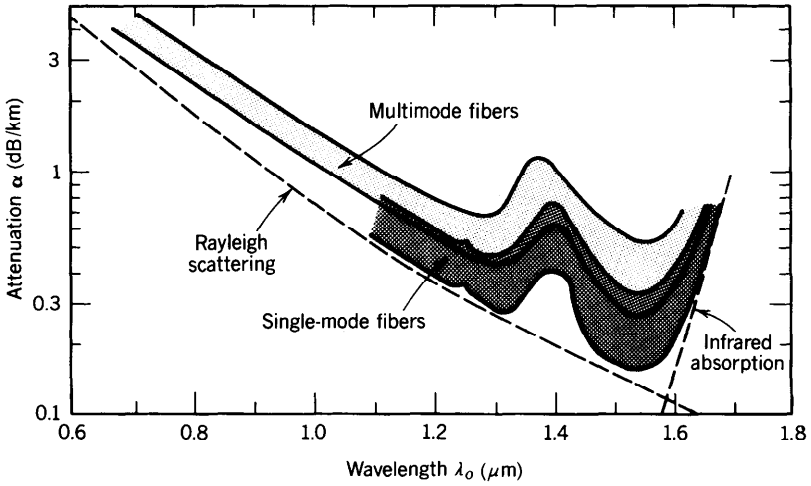


**Figure 8.3-3** Ranges of attenuation coefficients of silica glass single-mode and multimode fibers.

scattering of sunlight from tiny atmospheric molecules, is the reason the sky appears blue). The attenuation caused by Rayleigh scattering therefore decreases with wavelength as  $1/\lambda^4$ , a relation known as **Rayleigh’s inverse fourth-power law**. In the visible band, Rayleigh scattering is more significant than the tail of the ultraviolet absorption band, but it becomes negligible in comparison with infrared absorption for wavelengths greater than  $1.6 \mu\text{m}$ .

The transparent window in silica glass is therefore bounded by Rayleigh scattering on the short-wavelength side and by infrared absorption on the long-wavelength side (as indicated by the dashed lines in Fig. 8.3-2).

**Extrinsic Effects**

In addition to these intrinsic effects there are extrinsic absorption bands due to impurities, mainly OH vibrations associated with water vapor dissolved in the glass and metallic-ion impurities. Recent progress in the technology of fabricating glass fibers has made it possible to remove most metal impurities, but OH impurities are difficult to eliminate. Wavelengths at which glass fibers are used for optical communication are selected to avoid these absorption bands. Light-scattering losses may also be accentuated when dopants are added for the purpose of index grading, for example.

The attenuation coefficient of guided light in glass fibers depends on the absorption and scattering in the core and cladding materials. Since each mode has a different penetration depth into the cladding so that rays travel different effective distances, the attenuation coefficient is mode dependent. It is generally higher for higher-order modes. Single-mode fibers therefore typically have smaller attenuation coefficients than multimode fibers (Fig. 8.3-3). Losses are also introduced by small random variations in the geometry of the fiber and by bends.

**B. Dispersion**

When a short pulse of light travels through an optical fiber its power is “dispersed” in time so that the pulse spreads into a wider time interval. There are four sources of dispersion in optical fibers: modal dispersion, material dispersion, waveguide dispersion, and nonlinear dispersion.

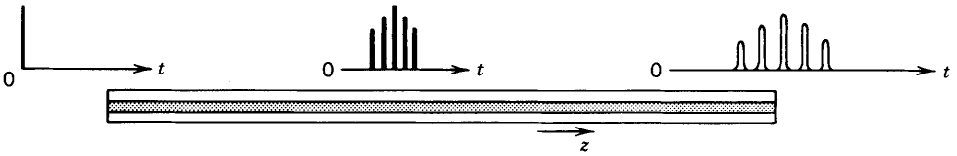


Figure 8.3-4 Pulse spreading caused by modal dispersion.

### Modal Dispersion

Modal dispersion occurs in multimode fibers as a result of the differences in the group velocities of the modes. A single impulse of light entering an  $M$ -mode fiber at  $z = 0$  spreads into  $M$  pulses with the differential delay increasing as a function of  $z$ . For a fiber of length  $L$ , the time delays encountered by the different modes are  $\tau_q = L/v_q$ ,  $q = 1, \dots, M$ , where  $v_q$  is the group velocity of mode  $q$ . If  $v_{\min}$  and  $v_{\max}$  are the smallest and largest group velocities, the received pulse spreads over a time interval  $L/v_{\min} - L/v_{\max}$ . Since the modes are generally not excited equally, the overall shape of the received pulse is a smooth profile, as illustrated in Fig. 8.3-4. An estimate of the overall rms pulse width is  $\sigma_\tau = \frac{1}{2}(L/v_{\min} - L/v_{\max})$ . This width represents the response time of the fiber.

In a step-index fiber with a large number of modes,  $v_{\min} \approx c_1(1 - \Delta)$  and  $v_{\max} \approx c_1$  (see Sec. 8.1B and Fig. 8.2-8). Since  $(1 - \Delta)^{-1} \approx 1 + \Delta$ , the response time is

$$\sigma_\tau \approx \frac{L \Delta}{c_1 2}, \quad (8.3-4)$$

Response Time  
(Multimode Step-Index Fiber)

i.e., it is a fraction  $\Delta/2$  of the delay time  $L/c_1$ .

Modal dispersion is much smaller in graded-index fibers than in step-index fibers since the group velocities are equalized and the differences between the delay times  $\tau_q = L/v_q$  of the modes are reduced. It was shown in Sec. 8.2B and in Fig. 8.2-8 that in a graded-index fiber with a large number of modes and with an optimal index profile,  $v_{\max} \approx c_1$  and  $v_{\min} \approx c_1(1 - \Delta^2/2)$ . The response time is therefore

$$\sigma_\tau \approx \frac{L \Delta^2}{c_1 4}, \quad (8.3-5)$$

Response Time  
(Graded-Index Fiber)

which is a factor of  $\Delta/2$  smaller than that in a step-index fiber.

---

**EXAMPLE 8.3-1. Multimode Pulse Broadening Rate.** In a step-index fiber with  $\Delta = 0.01$  and  $n = 1.46$ , pulses spread at a rate of approximately  $\sigma_\tau/L = \Delta/2c_1 = n_1\Delta/2c_0 \approx 24$  ns/km. In a 100-km fiber, therefore, an impulse spreads to a width of  $\approx 2.4$   $\mu$ s. If the same fiber is optimally index graded, the pulse broadening rate is approximately  $n_1\Delta^2/4c_0 \approx 122$  ps/km, which is substantially reduced.

---

The pulse broadening arising from modal dispersion is proportional to the fiber length  $L$  in both step-index and graded-index fibers. This dependence, however, does not necessarily hold when the fibers are longer than a certain critical length because of mode coupling. Coupling occurs between modes of approximately the same propagation constants as a result of small imperfections in the fiber (random irregularities of the fiber surface, or inhomogeneities of the refractive index) which permit the optical power to be exchanged between the modes. Under certain conditions, the response time  $\sigma_\tau$  of mode-coupled fibers is proportional to  $L$  for small  $L$  and to  $L^{1/2}$  when a critical length is exceeded, so that pulses are broadened at a slower rate<sup>†</sup>.

**Material Dispersion**

Glass is a dispersive medium; i.e, its refractive index is a function of wavelength. As discussed in Sec. 5.6, an optical pulse travels in a dispersive medium of refractive index  $n$  with a group velocity  $v = c_o/N$ , where  $N = n - \lambda_o \, dn/d\lambda_o$ . Since the pulse is a wavepacket, composed of a spectrum of components of different wavelengths each traveling at a different group velocity, its width spreads. The temporal width of an optical impulse of spectral width  $\sigma_\lambda$  (nm), after traveling a distance  $L$ , is  $\sigma_\tau = (d/d\lambda_o)(L/v)\sigma_\lambda = (d/d\lambda_o)(LN/c_o)\sigma_\lambda$ , from which

$$\sigma_\tau = |D_\lambda| \sigma_\lambda L, \tag{8.3-6}$$

Response Time  
(Material Dispersion)

where

$$D_\lambda = - \frac{\lambda_o}{c_o} \frac{d^2 n}{d\lambda_o^2} \tag{8.3-7}$$

is the material dispersion coefficient [see (5.6-21)]. The response time increases linearly with the distance  $L$ . Usually,  $L$  is measured in km,  $\sigma_\tau$  in ps, and  $\sigma_\lambda$  in nm, so that  $D_\lambda$  has units of ps/km-nm. This type of dispersion is called **material dispersion** (as opposed to modal dispersion).

The wavelength dependence of the dispersion coefficient  $D_\lambda$  for silica glass is shown in Fig. 8.3-5. At wavelengths shorter than 1.3  $\mu\text{m}$  the dispersion coefficient is negative,

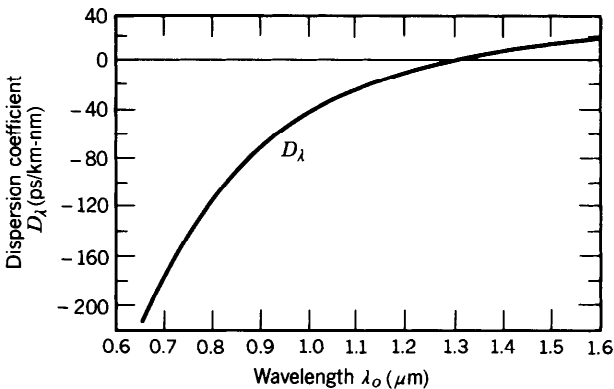


**Figure 8.3-5** The dispersion coefficient  $D_\lambda$  of silica glass as a function of wavelength  $\lambda_o$  (see also Fig. 5.6-5).

<sup>†</sup>See, e.g., J. E. Midwinter, *Optical Fibers for Transmission*, Wiley, New York, 1979.

so that wavepackets of long wavelength travel faster than those of short wavelength. At a wavelength  $\lambda_o = 0.87 \mu\text{m}$ , the dispersion coefficient  $D_\lambda$  is approximately  $-80 \text{ ps/km-nm}$ . At  $\lambda_o = 1.55 \mu\text{m}$ ,  $D_\lambda \approx +17 \text{ ps/km-nm}$ . At  $\lambda_o \approx 1.312 \mu\text{m}$  the dispersion coefficient vanishes, so that  $\sigma_\tau$  in (8.3-6) vanishes. A more precise expression for  $\sigma_\tau$  that incorporates the spread of the spectral width  $\sigma_\lambda$  about  $\lambda_o = 1.312 \mu\text{m}$  yields a very small, but nonzero, width.

---

**EXAMPLE 8.3-2. Pulse Broadening Associated with Material Dispersion.** The dispersion coefficient  $D_\lambda \approx -80 \text{ ps/km-nm}$  at  $\lambda_o \approx 0.87 \mu\text{m}$ . For a source of linewidth  $\sigma_\lambda = 50 \text{ nm}$  (from an LED, for example) the pulse spreading rate in a single-mode fiber with no other sources of dispersion is  $|D_\lambda|\sigma_\lambda = 4 \text{ ns/km}$ . An impulse of light traveling a distance  $L = 100 \text{ km}$  in the fiber is therefore broadened to a width  $\sigma_\tau = |D_\lambda|\sigma_\lambda L = 0.4 \mu\text{s}$ . The response time of the fiber is then  $0.4 \mu\text{s}$ . An impulse of narrower linewidth  $\sigma_\lambda = 2 \text{ nm}$  (from a laser diode, for example) operating near  $1.3 \mu\text{m}$ , where the dispersion coefficient is  $1 \text{ ps/km-nm}$ , spreads at a rate of only  $2 \text{ ps/km}$ . A 100-km fiber thus has a substantially shorter response time,  $\sigma_\tau = 0.2 \text{ ns}$ .

---

### Waveguide Dispersion

The group velocities of the modes depend on the wavelength even if material dispersion is negligible. This dependence, known as **waveguide dispersion**, results from the dependence of the field distribution in the fiber on the ratio between the core radius and the wavelength ( $a/\lambda_o$ ). If this ratio is altered, by altering  $\lambda_o$ , the relative portions of optical power in the core and cladding are modified. Since the phase velocities in the core and cladding are different, the group velocity of the mode is altered. Waveguide dispersion is particularly important in single-mode fibers, where modal dispersion is not exhibited, and at wavelengths for which material dispersion is small (near  $\lambda_o = 1.3 \mu\text{m}$  in silica glass).

As discussed in Sec. 8.1B, the group velocity  $v = (d\beta/d\omega)^{-1}$  and the propagation constant  $\beta$  are determined from the characteristic equation, which is governed by the fiber  $V$  parameter  $V = 2\pi(a/\lambda_o)\text{NA} = (a \cdot \text{NA}/c_o)\omega$ . In the absence of material dispersion (i.e., when NA is independent of  $\omega$ ),  $V$  is directly proportional to  $\omega$ , so that

$$\frac{1}{v} = \frac{d\beta}{d\omega} = \frac{d\beta}{dV} \frac{dV}{d\omega} = \frac{a \cdot \text{NA}}{c_o} \frac{d\beta}{dV}. \quad (8.3-8)$$

The pulse broadening associated with a source of spectral width  $\sigma_\lambda$  is related to the time delay  $L/v$  by  $\sigma_\tau = (d/d\lambda_o)(L/v)\sigma_\lambda$ . Thus

$$\sigma_\tau = |D_w|\sigma_\lambda L, \quad (8.3-9)$$

where

$$D_w = \frac{d}{d\lambda_o} \left( \frac{1}{v} \right) = -\frac{\omega}{\lambda_o} \frac{d}{d\omega} \left( \frac{1}{v} \right) \quad (8.3-10)$$

is the waveguide dispersion coefficient. Substituting (8.3-8) into (8.3-10) we obtain

$$D_w = - \left( \frac{1}{2\pi c_o} \right) V^2 \frac{d^2\beta}{dV^2}. \quad (8.3-11)$$

Thus the group velocity is inversely proportional to  $d\beta/dV$  and the dispersion coefficient is proportional to  $V^2 d^2\beta/dV^2$ . The dependence of  $\beta$  on  $V$  is shown in Fig. 8.1-10(b) for the fundamental  $LP_{01}$  mode. Since  $\beta$  varies nonlinearly with  $V$ , the waveguide dispersion coefficient  $D_w$  is itself a function of  $V$  and is therefore also a function of the wavelength.<sup>†</sup> The dependence of  $D_w$  on  $\lambda_o$  may be controlled by altering the radius of the core or the index grading profile for graded-index fibers.

### Combined Material and Waveguide Dispersion

The combined effects of material dispersion and waveguide dispersion (referred to here as **chromatic dispersion**) may be determined by including the wavelength dependence of the refractive indices,  $n_1$  and  $n_2$  and therefore NA, when determining  $d\beta/d\omega$  from the characteristic equation. Although generally smaller than material dispersion, waveguide dispersion does shift the wavelength at which the total chromatic dispersion is minimum.

Since chromatic dispersion limits the performance of single-mode fibers, more advanced fiber designs aim at reducing this effect by using graded-index cores with refractive-index profiles selected such that the wavelength at which waveguide dispersion compensates material dispersion is shifted to the wavelength at which the fiber is to be used. **Dispersion-shifted fibers** have been successfully made by using a linearly tapered core refractive index and a reduced core radius, as illustrated in Fig. 8.3-6(a). This technique can be used to shift the zero-chromatic-dispersion wavelength from 1.3  $\mu\text{m}$  to 1.55  $\mu\text{m}$ , where the fiber has its lowest attenuation. Note, however, that the process of index grading itself introduces losses since dopants are used. Other grading profiles have been developed for which the chromatic dispersion vanishes at two wavelengths and is reduced for wavelengths between. These fibers, called **dispersion-flattened**, have been implemented by using a quadruple-clad layered grading, as illustrated in Fig. 8.3-6(b).

### Combined Material and Modal Dispersion

The effect of material dispersion on pulse broadening in multimode fibers may be determined by returning to the original equations for the propagation constants  $\beta_q$  of the modes and determining the group velocities  $v_q = (d\beta_q/d\omega)^{-1}$  with  $n_1$  and  $n_2$  being functions of  $\omega$ . Consider, for example, the propagation constants of a graded-index fiber with a large number of modes, which are given by (8.2-19) and (8.2-15). Although  $n_1$  and  $n_2$  are dependent on  $\omega$ , it is reasonable to assume that the ratio  $\Delta = (n_1 - n_2)/n_1$  is approximately independent of  $\omega$ . Using this approximation and evaluating  $v_q = (d\beta_q/d\omega)^{-1}$ , we obtain

$$v_q \approx \frac{c_o}{N_1} \left[ 1 - \frac{p-2}{p+2} \left( \frac{q}{M} \right)^{p/(p+2)} \Delta \right], \quad (8.3-12)$$

where  $N_1 = (d/d\omega)(\omega n_1) = n_1 - \lambda_o (dn_1/d\lambda_o)$  is the group index of the core material. Under this approximation, the earlier expression (8.2-21) for  $v_q$  remains the same, except that the refractive index  $n_1$  is replaced with the group index  $N_1$ . For a step-index fiber ( $p = \infty$ ), the group velocities of the modes vary from  $c_o/N_1$  to

<sup>†</sup> For more details on this topic, see the reading list, particularly the articles by Gloge.

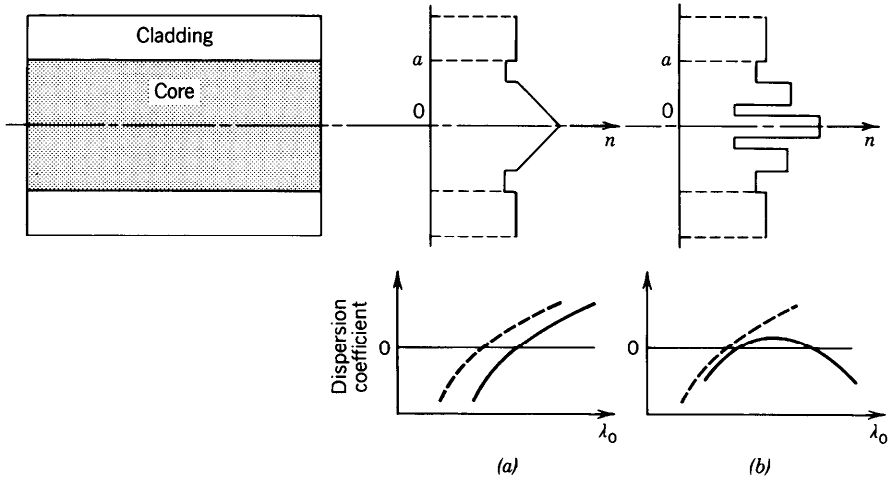


**Figure 8.3-6** Refractive-index profiles and schematic wavelength dependences of the material dispersion coefficient (dashed curves) and the combined material and waveguide dispersion coefficients (solid curves) for (a) dispersion-shifted and (b) dispersion-flattened fibers.

$(c_o/N_1)(1 - \Delta)$ , so that the response time is

$$\sigma_\tau \approx \frac{L}{(c_o/N_1)} \frac{\Delta}{2}$$

(8.3-13)  
Response Time  
(Multimode Step-Index Fiber  
with Material Dispersion)

This should be compared with (8.3-4) when there is no material dispersion.

**EXERCISE 8.3-1**

**Optimal Grade Profile Parameter.** Use (8.2-19) and (8.2-15) to derive the following expression for the group velocity  $v_q$  when both  $n_1$  and  $\Delta$  are wavelength dependent:

$$v_q \approx \frac{c_o}{N_1} \left[ 1 - \frac{p-2-p_s}{p+2} \left( \frac{q}{M} \right)^{p/(p+2)} \Delta \right], \quad q = 1, 2, \dots, M, \quad (8.3-14)$$

where  $p_s = 2(n_1/N_1)(\omega/\Delta) d\Delta/d\omega$ . What is the optimal value of the grade profile parameter  $p$  for minimizing modal dispersion?

**Nonlinear Dispersion**

Yet another dispersion effect occurs when the intensity of light in the core is sufficiently high, since the refractive indices then become intensity dependent and the material exhibits nonlinear behavior. The high-intensity parts of an optical pulse undergo phase shifts different from the low-intensity parts, so that the frequency is shifted by different amounts. Because of material dispersion, the group velocities are

modified, and consequently the pulse shape is altered. Under certain conditions, nonlinear dispersion can compensate material dispersion, so that the pulse travels without altering its temporal profile. The guided wave is then known as a solitary wave, or a soliton. Nonlinear optics is introduced in Chap. 19 and optical solitons are discussed in Sec. 19.8.

### C. Pulse Propagation

As described in the previous sections, the propagation of pulses in optical fibers is governed by attenuation and several types of dispersion. The following is a summary and recapitulation of these effects, ignoring nonlinear dispersion.

An optical pulse of power  $\tau_0^{-1}\rho(t/\tau_0)$  and short duration  $\tau_0$ , where  $\rho(t)$  is a function which has unit duration and unit area, is transmitted through a multimode fiber of length  $L$ . The received optical power may be written in the form of a sum

$$P(t) \propto \sum_{q=1}^M \exp(-0.23\alpha_q L) \sigma_q^{-1} \rho\left(\frac{t - \tau_q}{\sigma_q}\right), \tag{8.3-15}$$

where  $M$  is the number of modes, the subscript  $q$  refers to mode  $q$ ,  $\alpha_q$  is the attenuation coefficient (dB/km),  $\tau_q = L/v_q$  is the delay time,  $v_q$  is the group velocity, and  $\sigma_q > \tau_0$  is the width of the pulse associated with mode  $q$ . In writing (8.3-15), we have implicitly assumed that the incident optical power is distributed equally among the  $M$  modes of the fiber. It has also been assumed that the pulse shape  $\rho(t)$  is not altered; it is only delayed by times  $\tau_q$  and broadened to widths  $\sigma_q$  as a result of propagation. As was shown in Sec. 5.6, an initial pulse with a Gaussian profile is indeed broadened without altering its Gaussian nature.

The received pulse is thus composed of  $M$  pulses of widths  $\sigma_q$  centered at time delays  $\tau_q$ , as illustrated in Fig. 8.3-7. The composite pulse has an overall width  $\sigma_\tau$  which represents the overall response time of the fiber.

We therefore identify two basic types of dispersion: **intermodal** and **intramodal**. Intermodal, or simply modal, dispersion is the delay distortion caused by the disparity among the delay times  $\tau_q$  of the modes. The time difference  $\frac{1}{2}(\tau_{\max} - \tau_{\min})$  between the longest and shortest delay constitutes modal dispersion. It is given by (8.3-4) and (8.3-5) for step-index and graded-index fibers with a large number of modes, respectively. Material dispersion has some effect on modal dispersion since it affects the delay times. For example, (8.3-13) gives the modal dispersion of a multimode fiber with material dispersion. Modal dispersion is directly proportional to the fiber length  $L$ , except for long fibers, in which mode coupling plays a role, whereupon it becomes proportional to  $L^{1/2}$ .

Intramodal dispersion is the broadening of the pulses associated with the individual modes. It is caused by a combination of material dispersion and waveguide dispersion

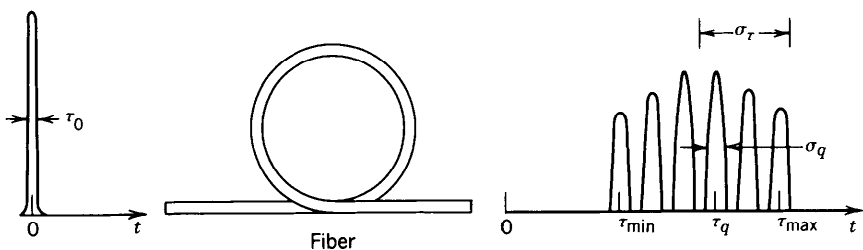
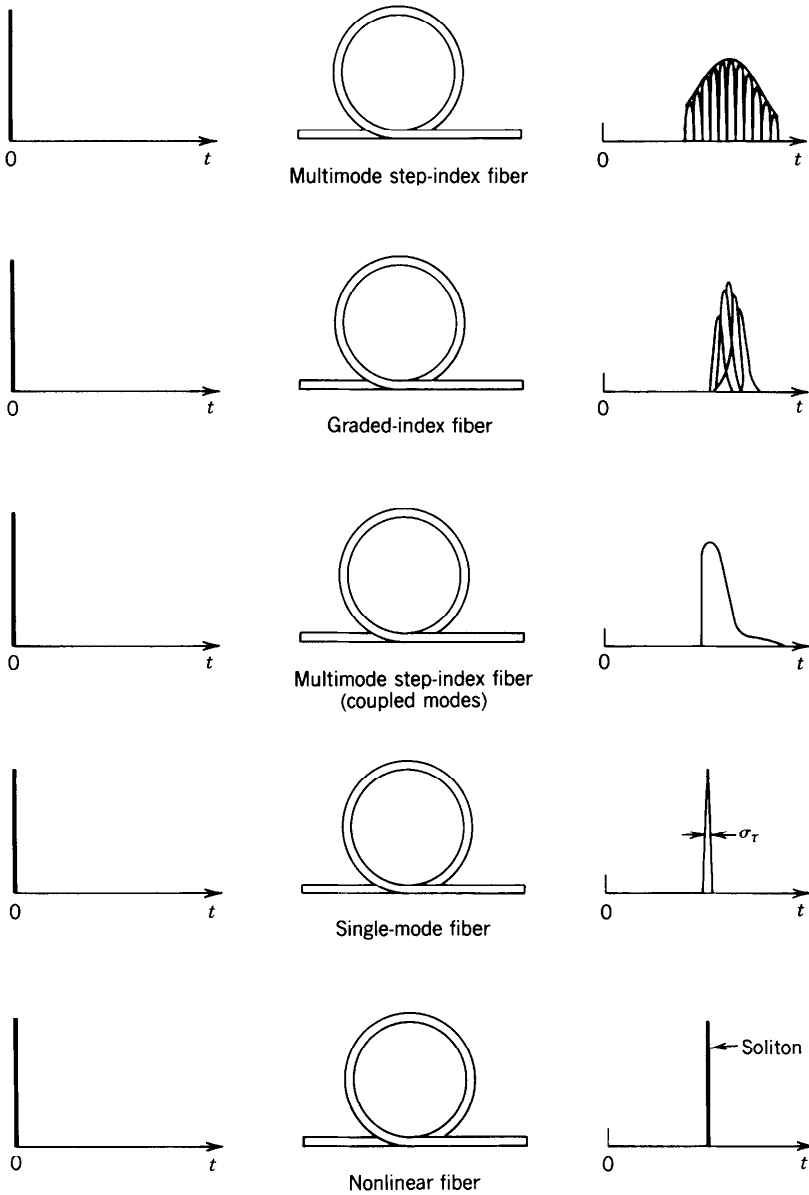


Figure 8.3-7 Response of a multimode fiber to a single pulse.



**Figure 8.3-8** Broadening of a short optical pulse after transmission through different types of fibers. The width of the transmitted pulse is governed by modal dispersion in multimode (step-index and graded-index) fibers. In single-mode fibers the pulse width is determined by material dispersion and waveguide dispersion. Under certain conditions an intense pulse, called a soliton, can travel through a nonlinear fiber without broadening. This is a result of a balance between material dispersion and self-phase modulation (the dependence of the refractive index on the light intensity).

resulting from the finite spectral width of the initial optical pulse. The width  $\sigma_q$  is given by

$$\sigma_q^2 \approx \tau_0^2 + (D_q \sigma_\lambda L)^2, \quad (8.3-16)$$

where  $D_q$  is a dispersion coefficient representing the combined effects of material and waveguide dispersion for mode  $q$ . Material dispersion is usually more significant. For a very short initial width  $\tau_0$ , (8.3-16) gives

$$\sigma_q \approx D_q \sigma_\lambda L. \quad (8.3-17)$$

Figure 8.3-8 is a schematic illustration in which the profiles of pulses traveling through different types of fibers are compared. In multimode step-index fibers, the modal dispersion  $\frac{1}{2}(\tau_{\max} - \tau_{\min})$  is usually much greater than the material/waveguide dispersion  $\sigma_q$ , so that intermodal dispersion dominates and  $\sigma_\tau \approx \frac{1}{2}(\tau_{\max} - \tau_{\min})$ . In multimode graded-index fibers,  $\frac{1}{2}(\tau_{\max} - \tau_{\min})$  may be comparable to  $\sigma_q$ , so that the overall pulse width involves all dispersion effects. In single-mode fibers, there is obviously no modal dispersion and the transmission of pulses is limited by material and waveguide dispersion. The lowest overall dispersion is achieved in a single-mode fiber operating at the wavelength for which the combined material-waveguide dispersion vanishes.

## READING LIST

### Books

See also the books on optical waveguides in Chapter 7.

- P. K. Cheo, *Fiber Optics and Optoelectronics*, Prentice Hall, Englewood Cliffs, NJ, 1985, 2nd ed. 1990.
- F. C. Allard, *Fiber Optics Handbook for Engineers and Scientists*, McGraw-Hill, New York, 1990.
- C. Yeh, *Handbook of Fiber Optics: Theory and Applications*, Academic Press, Orlando, FL, 1990.
- L. B. Jeunhomme, *Single-Mode Fiber Optics*, Marcel Dekker, New York, 1983, 2nd ed. 1990.
- P. W. France, ed., *Fluoride Glass Optical Fibers*, CRC Press, Boca Raton, FL, 1989.
- P. Diamant, *Wave Transmission and Fiber Optics*, Macmillan, New York, 1989.
- W. B. Jones, Jr., *Introduction to Optical Fiber Communication Systems*, Holt, Rinehart and Winston, New York, 1988.
- H. Murata, *Handbook of Optical Fibers and Cables*, Marcel Dekker, New York, 1988.
- E. G. Neuman, *Single-Mode Fibers—Fundamentals*, Springer-Verlag, New York, 1988.
- E. L. Safford, Jr. and J. A. McCann, *Fiberoptics and Laser Handbook*, Tab Books, Blue Ridge Summit, PA, 2nd ed. 1988.
- S. E. Miller and I. Kaminow, *Optical Fiber Telecommunications II*, Academic Press, Boston, MA, 1988.
- J. Gowar, *Optical Communication Systems*, Prentice Hall, Englewood Cliffs, NJ, 1984.
- R. G. Seippel, *Fiber Optics*, Reston Publishing, Reston, VA, 1984.
- ANSI/IEEE Standards 812-1984, *IEEE Standard Definitions of Terms Relating to Fiber Optics*, IEEE, New York, 1984.
- A. H. Cherin, *An Introduction to Optical Fibers*, McGraw-Hill, New York, 1983.
- G. E. Keiser, *Optical Fiber Communications*, McGraw-Hill, New York, 1983.
- C. Hentschel, *Fiber Optics Handbook*, Hewlett-Packard, Palo Alto, CA, 1983.
- Y. Suematsu and K. Iga, *Introduction to Optical Fiber Communications*, Wiley, New York, 1982.
- T. Okoshi, *Optical Fibers*, Academic Press, New York, 1982.
- C. K. Kao, *Optical Fiber Systems*, McGraw-Hill, New York, 1982.
- E. A. Lacy, *Fiber Optics*, Prentice-Hall, Englewood Cliffs, NJ, 1982.

- D. Marcuse, *Light Transmission Optics*, Van Nostrand Reinhold, New York, 1972, 2nd ed. 1982.
- D. Marcuse, *Principles of Optical Fiber Measurements*, Academic Press, New York, 1981.
- A. B. Sharma, S. J. Halme, and M. M. Butusov, *Optical Fiber Systems and Their Components*, Springer-Verlag, Berlin, 1981.
- CSELT (Centro Studi e Laboratori Telecomunicazioni), *Optical Fibre Communications*, McGraw-Hill, New York, 1981.
- M. K. Barnoski, ed., *Fundamentals of Optical Fiber Communications*, Academic Press, New York, 1976, 2nd ed. 1981.
- C. P. Sandbank, ed., *Optical Fibre Communication Systems*, Wiley, New York, 1980.
- M. J. Howes and D. V. Morgan, eds., *Optical Fibre Communications*, Wiley, New York, 1980.
- H. F. Wolf, ed., *Handbook of Fiber Optics*, Garland STPM Press, New York, 1979.
- D. B. Ostrowsky, ed., *Fiber and Integrated Optics*, Plenum Press, New York, 1979.
- J. E. Midwinter, *Optical Fibers for Transmission*, Wiley, New York, 1979.
- S. E. Miller and A. G. Chynoweth, *Optical Fiber Telecommunications*, Academic Press, New York, 1979.
- G. R. Elion and H. A. Elion, *Fiber Optics in Communication Systems*, Marcel Dekker, New York, 1978.
- H. G. Unger, *Planar Optical Waveguides and Fibers*, Clarendon Press, Oxford, 1977.
- J. A. Arnaud, *Beam and Fiber Optics*, Academic Press, New York, 1976.
- W. B. Allan, *Fibre Optics: Theory and Practice*, Plenum Press, New York, 1973.
- N. S. Kapany, *Fiber Optics: Principles and Applications*, Academic Press, New York, 1967.

### Special Journal Issues

- Special issue on fiber-optic sensors, *Journal of Lightwave Technology*, vol. LT-5, no. 7, 1987.
- Special issue on fiber, cable, and splicing technology, *Journal of Lightwave Technology*, vol. LT-4, no. 8, 1986.
- Special issue on low-loss fibers, *Journal of Lightwave Technology*, vol. LT-2, no. 10, 1984.
- Special issue on fiber optics, *IEEE Transactions on Communications*, vol. COM-26, no. 7, 1978.

### Articles

- M. G. Drexhage and C. T. Moynihan, Infrared Optical Fibers, *Scientific American*, vol. 259, no. 5, pp. 110–114, 1988.
- S. R. Nagel, Optical Fiber—the Expanding Medium, *IEEE Communications Magazine*, vol. 25, no. 4, pp. 33–43, 1987.
- R. H. Stolen and R. P. DePaula, Single-Mode Fiber Components, *Proceedings of the IEEE*, vol. 75, pp. 1498–1511, 1987.
- P. S. Henry, Lightwave Primer, *IEEE Journal of Quantum Electronics*, vol. QE-21, pp. 1862–1879, 1985.
- T. Li, Advances in Optical Fiber Communications: An Historical Perspective, *IEEE Journal on Selected Areas in Communications*, vol. SAC-1, pp. 356–372, 1983.
- I. P. Kaminow, Polarization in Optical Fibers, *IEEE Journal of Quantum Electronics*, vol. QE-17, pp. 15–22, 1981.
- P. J. B. Clarricoats, Optical Fibre Waveguides—A Review, in *Progress in Optics*, vol. 14, E. Wolf, ed., North-Holland, Amsterdam, 1977.
- D. Gloge, Weakly Guiding Fibers, *Applied Optics*, vol. 10, pp. 2252–2258, 1971.
- D. Gloge, Dispersion in Weakly Guiding Fibers, *Applied Optics*, vol. 10, pp. 2442–2445, 1971.

## PROBLEMS

- 8.1-1 **Coupling Efficiency.** (a) A source emits light with optical power  $P_0$  and a distribution  $I(\theta) = (1/\pi)P_0 \cos \theta$ , where  $I(\theta)$  is the power per unit solid angle in the direction making an angle  $\theta$  with the axis of a fiber. Show that the power collected

by the fiber is  $P = (\text{NA})^2 P_0$ , i.e., the coupling efficiency is  $\text{NA}^2$  where NA is the numerical aperture of the fiber.

(b) If the source is a planar light-emitting diode of refractive index  $n_s$  bonded to the fiber, and assuming that the fiber cross-sectional area is larger than the LED emitting area, calculate the numerical aperture of the fiber and the coupling efficiency when  $n_1 = 1.46$ ,  $n_2 = 1.455$ , and  $n_s = 3.5$ .

- 8.1-2 **Modes.** A step-index fiber has radius  $a = 5 \mu\text{m}$ , core refractive index  $n_1 = 1.45$ , and fractional refractive-index change  $\Delta = 0.002$ . Determine the shortest wavelength  $\lambda_c$  for which the fiber is a single-mode waveguide. If the wavelength is changed to  $\lambda_c/2$ , identify the indices  $(l, m)$  of all the guided modes.
- 8.1-3 **Modal Dispersion.** A step-index fiber of numerical aperture  $\text{NA} = 0.16$ , core radius  $a = 45 \mu\text{m}$  and core refractive index  $n_1 = 1.45$  is used at  $\lambda_o = 1.3 \mu\text{m}$ , where material dispersion is negligible. If a pulse of light of very short duration enters the fiber at  $t = 0$  and travels a distance of 1 km, sketch the shape of the received pulse: (a) Using ray optics and assuming that only meridional rays are allowed. (b) Using wave optics and assuming that only meridional ( $l = 0$ ) modes are allowed.
- 8.1-4 **Propagation Constants and Group Velocities.** A step-index fiber with refractive indices  $n_1 = 1.444$  and  $n_2 = 1.443$  operates at  $\lambda_o = 1.55 \mu\text{m}$ . Determine the core radius at which the fiber  $V$  parameter is 10. Use Fig. 8.1-6 to estimate the propagation constants of all the guided modes with  $l = 0$ . If the core radius is now changed so that  $V = 4$ , use Fig. 8.1-10(b) to determine the propagation constant and the group velocity of the  $\text{LP}_{01}$  mode. *Hint:* Derive an expression for the group velocity  $v = (d\beta/d\omega)^{-1}$  in terms of  $d\beta/dV$  and use Fig. 8.1-10(b) to estimate  $d\beta/dV$ . Ignore the effect of material dispersion.
- 8.2-1 **Numerical Aperture of a Graded-Index Fiber.** Compare the numerical apertures of a step-index fiber with  $n_1 = 1.45$  and  $\Delta = 0.01$  and a graded-index fiber with  $n_1 = 1.45$ ,  $\Delta = 0.01$ , and a parabolic refractive-index profile ( $p = 2$ ). (See Exercise 1.3-2 on page 24.)
- 8.2-2 **Propagation Constants and Wavevector (Step-Index Fiber).** A step-index fiber of radius  $a = 20 \mu\text{m}$  and refractive indices  $n_1 = 1.47$  and  $n_2 = 1.46$  operates at  $\lambda_o = 1.55 \mu\text{m}$ . Using the quasi-plane wave theory and considering only guided modes with azimuthal index  $l = 1$ : (a) Determine the smallest and largest propagation constants. (b) For the mode with the smallest propagation constant, determine the radii of the cylindrical shell within which the wave is confined, and the components of the wavevector  $\mathbf{k}$  at  $r = 5 \mu\text{m}$ .
- 8.2-3 **Propagation Constants and Wavevector (Graded-Index Fiber).** Repeat Problem 8.2-2 for a graded-index fiber with parabolic refractive-index profile with  $p = 2$ .
- 8.3-1 **Scattering Loss.** At  $\lambda_o = 820 \text{ nm}$  the absorption loss of a fiber is 0.25 dB/km and the scattering loss is 2.25 dB/km. If the fiber is used instead at  $\lambda_o = 600 \text{ nm}$  and calorimetric measurements of the heat generated by light absorption give a loss of 2 dB/km, estimate the total attenuation at  $\lambda_o = 600 \text{ nm}$ .
- 8.3-2 **Modal Dispersion in Step-Index Fibers.** Determine the core radius of a multimode step-index fiber with a numerical aperture  $\text{NA} = 0.1$  if the number of modes  $M = 5000$  when the wavelength is  $0.87 \mu\text{m}$ . If the core refractive index  $n_1 = 1.445$ , the group index  $N_1 = 1.456$ , and  $\Delta$  is approximately independent of wavelength, determine the modal-dispersion response time  $\sigma_r$  for a 2-km fiber.
- 8.3-3 **Modal Dispersion in Graded-Index Fibers.** Consider a graded-index fiber with  $a/\lambda_o = 10$ ,  $n_1 = 1.45$ ,  $\Delta = 0.01$ , and a power-law profile with index  $p$ . Determine

the number of modes  $M$ , and the modal-dispersion pulse-broadening rate  $\sigma_\tau/L$  for  $p = 1.9, 2, 2.1$ , and  $\infty$ .

- 8.3-4 **Pulse Propagation.** A pulse of initial width  $\tau_0$  is transmitted through a graded-index fiber of length  $L$  kilometers and power-law refractive-index profile with profile index  $p$ . The peak refractive index  $n_1$  is wavelength-dependent with  $D_\lambda = -(\lambda_o/c_o)d^2n_1/d\lambda_o^2$ ,  $\Delta$  is approximately independent of wavelength,  $\sigma_\lambda$  is the source's spectral width, and  $\lambda_o$  is the operating wavelength. Discuss the effect of increasing each of the following parameters on the width of the received pulse:  $L$ ,  $\tau_0$ ,  $p$ ,  $|D_\lambda|$ ,  $\sigma_\lambda$ , and  $\lambda_o$ .